Sensing and Bio-Sensing Research 38 (2022) 100540

Contents lists available at ScienceDirect

Sensing and Bio-Sensing Research

journal homepage: www.elsevier.com/locate/sbsr

2D Materials towards sensing technology: From fundamentals to applications

Manuel Vázquez Sulleiro [a,*], Antonio Dominguez-Alfaro [b], Nuria Alegret [c], Alessandro Silvestri [c], I. Jénnifer Gómez [d,*]

[a] IMDEA Nanociencia, Ciudad Universitaria de Cantoblanco, 28049 Madrid, Spain
[b] POLYMAT University of the Basque Country UPV/EHU, 20018 Donostia-San Sebastián, Spain
[c] Center for Cooperative Research in Biomaterials (CIC biomaGUNE), Basque Research and Technology Alliance (BRTA), 20014 Donostia-San Sebastián, Spain
[d] Department of Condensed Matter Physics, Faculty of Science, Masaryk University, 61137 Brno, Czech Republic

ARTICLE INFO

Keywords:
2D materials
Physical sensors
Chemical sensors
Biosensors and wearable sensors

ABSTRACT

2D materials raised extensive attention for physical-, chemical- and wearable-sensors, among others. The principal reason is the outstanding capability of 2D materials to detect specific analytes and physical stimuli through diverse responses. After a short introduction to 2D materials, a critical explanation of sensors containing 2D materials is provided to justify their applications. Following by a description of the most relevant transduction mechanisms of 2D materials employed for sensing. This review explores their advancement and implementation in sensing during the last decade in several areas, such as physical, chemical, bio and wearable sensors. Different types of 2D materials, including graphene, transition metal dichalcogenides (TMDs), hexagonal boron nitride (h-BN), 2D carbides and nitrides of transition metals (MXenes) and black phosphorus (BP), are considered.

1. Introduction

In a scenario where industrial globalization and population growth are raising public exposure to biological, chemical, and physical threats, nano-sensors are leading into a new era of ultrasensitive and real-time monitoring [1,2]. Therefore, it is imperative to seek easy, rapid, sensitive, user-friendly, selective and affordable in-cost sensors [3]. The detection and monitoring of temperature, current, radiation, chemicals, biomarkers and pathogens have been a challenge worldwide. The application of 2D materials in sensors is growing exponentially, from environmental monitoring to healthcare, due to their unique properties arising from their inherent structures [4].

Reviews on 2D materials have been presented so far, e.g., microfluid sensors [5], sensing technology toward health and environmental monitoring applications [3,6,7]. Although, most of these are dedicated to a specific type of 2D material or contrary to a particular sensing application. Herein, we review the state-of-the-art of the most-well know 2D materials-based sensors such as graphene, TMDs, h-BN, MXenes and BP (Fig. 1). In particular, we highlight the distinct properties of 2D materials that make them attractive and unique in the sensing field, with a critical comparison between sensors containing and non-containing 2D materials. Furthermore, we remark on the synthetic and engineering methods to produce them. An overview of the transduction sensing mechanisms is presented: electrochemical, electrical, piezoelectric and optical systems. To conclude, some of the most relevant examples in the last decade, with an essential focus on the previous five years, are reviewed in the field of physical, chemical, healthcare and wearable technologies.

2. Why 2D materials for sensing?

2D materials, including graphene, transition metal dichalcogenides (TMDs), black phosphorus (BP), hexagonal boron nitride (h-BN) and MXenes, have attracted significant attention in several fields, mainly in detection and sensing strategies [5]. Several are the benefits of 2D materials in this field. In the first instance, 2D materials are ideally single-layer materials with a thickness of a few nanometers, which imparts a remarkably high surface-area-to-volume ratio [8]. As a result, it provides numerous reactive sites between the material and analytes [9,10]. Furthermore, the conductivity of 2D materials can be tuned by controlling structural defects, increasing the number of layers, doping or even post-functionalizing the material [11]. Finally, 2D nanomaterials,

* Corresponding authors.
E-mail addresses: manuel.vazquez@imdea.org (M.V. Sulleiro), jennifer.gomez@mail.muni.cz (I.J. Gómez).

https://doi.org/10.1016/j.sbsr.2022.100540
Received 16 July 2022; Received in revised form 15 October 2022; Accepted 24 October 2022
Available online 25 October 2022

due to their mechanical strength and flexibility, are compatible with state-of-the-art technologies, such as ultrathin silicon channels [12,13], printing methods [14], metal electrodes [15], and flexible and wearable electronics [16].

The exponential increase in the number of publications studying the applicability of 2D materials in combination with the current sensing technologies testifies to their great potential in the field (Fig. 2) [12]. In the following paragraphs of the review, we will present a brief summary of the 2D materials studied in this area of research and a critical justification of the 2D materials benefits with their corresponding tuning approaches to enhanced sensing performance.

Graphene, the most studied 2D material, presents a single layer honeycomb crystalline structure of sp2 hybridized carbon atoms [8]. Graphene exhibits many excellent properties: high thermal conductivity and density, flexibility, mechanical strength, and optical transparency [17–19]. These properties can be modified with post-functionalization to tune and adapt the material to the desired application [20,21]. Graphene, and many other 2D materials, can be produced by two main approaches: bottom-up and top-down. Top-down approaches typically consist of the exfoliation of graphite into small flakes of graphene, and they comprise liquid phase exfoliation (LPE), mechanical exfoliation (ME), and electrochemical exfoliation (EE) [8,22]. The great advantages of exfoliated graphene are the solubility, liquid processability and low cost of production, while it is affected by some drawbacks such as an elevated number of defects, reduced conductivity and optical opacity. On the other side, the two most widespread bottom-up approaches are chemical vapour deposition (CVD) and epitaxial growth [23]. These strategies provide monolayer graphene with highly controlled chemical composition and crystalline structure, elevated conductivity and optical transparency [24].

TMDs are semiconductors formed by transition metals and elements from group-VI, depicted as formula MX_2, where M is a transition metal (e.g., Mo, W Ti, Nb) and X can be S, Se or Te [25–27]. M atoms are arranged in one plane surrounded by two planes of X through a covalent bond. TMDs presented unique chemical and physical properties such as high charge mobility, layer-dependent bandgaps, absorption, and emission of light [28]. The current applications of TMDs span from photonics and sensing to optoelectronics applications [29–32]. Analogously to graphene, TMDs can be produced by ME, LPE, and CVD deposition [33]. An interesting feature of TMDs, and in particular of molybdenum disulfide (MoS_2), is that the crystalline structure of the 2D material can be changed from 2H to 1T through ion intercalation method in the exfoliation process [33,34].

BP was first synthesized in 1914, but it was not until the last decade that it attracted tremendous attention [35,36]. BP is a layered semiconductor material in which individual atomic layers are stacked together by van der Waals interactions. Each phosphorus atom is covalently bonded with three adjacent phosphorus atoms to form a puckered honeycomb structure [37]. Its direct bandgap, distinctive wrinkled structure, high-hole mobility, excellent mechanical, electrical,

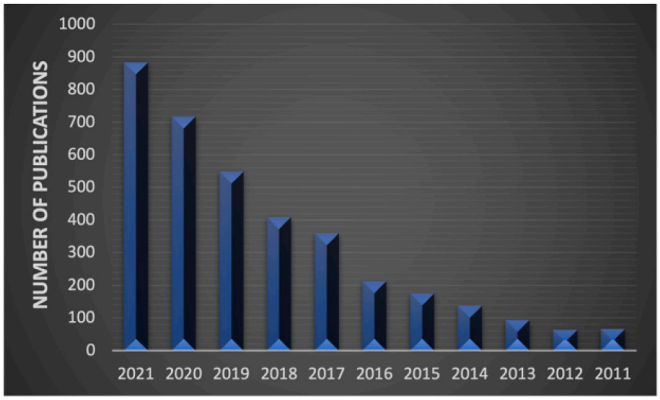

Fig. 2. Number of publications per year under the topics by Web of Science: Sensors with 2D materials, Graphene, MXenes, TMDCs, Black phosphorous, Boron nitride in the period 2021-2011.

and optical properties make BP a promising material for many applications. Although, its poor stability and fast chemical degradation under ambient conditions limit its use in many fields. Recently, BP was used for energy storage devices [38], photocatalysis [39], sensing and biomedical applications [40–44]. The most typically used protocol to produce few-layer BP is based on liquid-phase exfoliation and CVD [45,46].

h-BN presents a honeycomb hexagonal structure similar to graphene, where the boron and nitrogen atoms are presented in a 2D plane bonded *via* sp^2 [47]. Their specific properties, such as high mechanical, thermal and chemical stability, near-transparency, wide bandgap, and low dielectric constant turn this inorganic material into one of the most promising of the century, with possible applications from aerospace to medicine [48–51]. Generally, h-BN could be obtained by diverse top-down and bottom-up approaches [52], being the exfoliation method widely applied to obtain a single atomic plane with outstanding chemical stability, even in monolayer form [53].

MXenes are made from transition metal carbides and/or carbonitrides, and their first appearance in the research community was in 2011 [54]. MXenes are labelled with the formula $M_{n+1}AX_n$, where M refers to a transition metal (Ti, Mo, Cr, Nb, V, Sc, Zr, Hf or Ta), A stands for Al, Si, Sn, In, and X for carbon and/or nitrogen, and n could be equal to 1, 2, or 3. Due to their richness in chemical and morphological structures, hydrophilic nature and good electronic conductivity, MXenes could be considered optimal candidates for several applications from energy storage to photocatalysis and biomedicine [55]. Regarding their production, MXenes are synthesized by exfoliation through selective etching of the A layer from the MAX phase [56]: strong acid etching solutions containing aqueous fluoride (e.g., HF) are typically used [57].

The way in which 2D materials can improve the performances and the sensitivity of sensors is strongly dependent on the type of sensor considered, the transduction mechanism and the nature of the 2D

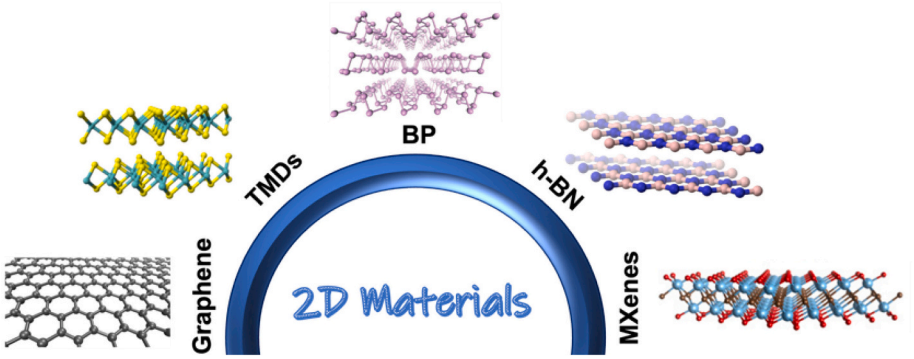

Fig. 1. Major classes of 2D materials considered in this review: Graphene, TMDs, BP, h-BN and MXenes.

material. Generally speaking, 2D materials provide a large surface area available to interact with the analyte, which permits the achievement of elevated sensitivity and ultra-low limits of detection. Furthermore, their surface is enriched with active sites that favor the interaction with targeted species or the immobilization of additional recognition components, such as metallic nanoparticles or bioreceptors, which can further enhance the sensing performance of the device. Another property characteristic of graphene and other 2D materials that enhances sensitivity, mainly in electrically transduced sensors, is conductivity: the electron transport, confined in the 2D plane, induces remarkable electronic properties [58].

For instance, the application of 2D materials in electrochemical sensors can have several advantages that ultimately improve the sensitivity and selectivity of the device. The large surface area and good electron mobility are factors fundamental in determining the selectivity of these materials. Furthermore, the presence of active sites provides these materials electrocatalytic properties that improve the registered currents while reducing the redox potential in the presence of the analyte. Wang *et al.* demonstrated that glassy carbon electrodes modified with graphene could decrease the reduction potential of H_2O_2 by approximately 0.4 V while improving 20 times the faradaic current [59]. Furthermore, they demonstrated that the doping of graphene with heteroatoms could tune the electrocatalytic properties of the material, improving further the electrode performances. As a result, electrodes modified with graphene and N-doped graphene demonstrated tremendous sensitivity in the detection of f H_2O_2 and Glucose. Silvestri *et al.* demonstrated as well that the incorporation of graphene in enzymatic sensors could improve 4 folds the sensitivity of the device [60].

In the case of gas sensing, several characteristics of 2D materials help explain their excellent sensing performance. Due to the 2D geometry, the whole surface of these materials is available to adsorb the gases, maximizing their interaction with the surface. The high crystallinity, together with the elevated conductivity, ensures noise reduction. Finally, graphene can be easily integrated with diverse device architectures with low resistance ohmic contacts. Based on these principles, Novoselov and coworkers presented a highly sensitive sensor made from graphene that can detect a single gas molecule interacting with the surface [61]. The authors demonstrated that graphene is an electronically quiet 2D material that can be used in single-electron detectors.

Different properties dictate the extremely high sensitivity of 2D material-based strain sensors. The layered structure characteristic of exfoliated 2D materials and the sub-nanometric gaps present among the layers provide unique piezoelectric properties with elevated gauge factors (GF). As a result, devices based on 2D materials present an extremely high sensitivity, allowing the detection of the weakest mechanical forces [62].

Surface modification or functionalization approaches (*i.e.*, chemical) to enhance the sensing performance of 2D materials are mainly classified into covalent and non-covalent approaches (Fig. 3) [63–68]. Covalent approaches are considered robust and allow attaching functional groups to the surface of the 2D materials, leading to tuning their electronic properties and modifying their crystal structure [69–71]. However, the modification of their surface, while effective in selectivity, can disrupt the electronic character making them poor candidates for sensing. Oppositely using the versatile non-covalent functionalization, the electronic and physical properties of the 2D materials can be changed without interfering with their crystal structure. In addition, non-covalent approaches of 2D materials can be carried out *via* van der Waals, electrostatic and π -π interactions, which can be used to tune doping levels controllably.

3. Transduction sensing mechanisms for 2D materials

A sensor is a system or device that detects, monitors and responds to multiple inputs and converts them into a particular form that can result in perception (*i.e.*, readout). In detail, sensors transform these

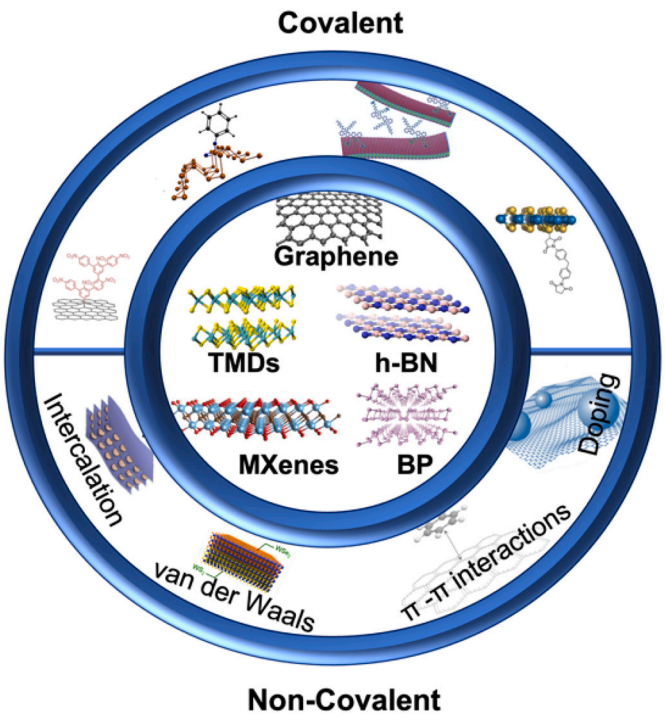

Fig. 3. Engineering 2D materials to achieve enhanced sensing performance *via* covalent and non-covalent approaches.

variations, with a specific mechanism, into a marker to monitor the device variable. In the next paragraph, we provide the featured principles of the standard transduction mechanisms of 2D materials employed for sensing: electrochemical, electrical, piezoelectric and optical (Fig. 4). Specific examples will be detailed in Section 4: Sensing applications.

3.1. Electrochemical mechanism

Electrochemical sensors are a class of sensors in which an electrode is used as a transducer element in the presence of an analyte. Electrochemical sensors, thanks to their innate accuracy, specificity, sensitivity, fast response, and easy-to-use set-up, are a popular choice among analytic platforms [72]. Electrochemical sensors detect electrochemical reactions happening between the electrode surface and the analytes. They typically convert chemical concentrations into quantitative electric signals. Electrochemical sensors are generally based on amperometry, potentiometry and conductometric measurements. Thus, quantitative detection of an electrochemical signal (*i.e.*, electron transfer of a particular analyte, oxidation or reduction) can be improved *via* a specific design of the working electrode modified with 2D materials [73]. Albeit not all analytes can induce redox reactions, in those cases, external mediators are needed to generate an electrochemical signal proportional to the analyte concentration [74].

In this section, we would like to highlight two of the most diffused electrochemical sensors, voltammetric and amperometric [75,76]. Voltammetric sensors measure the current in function of the potential variation while redox reactions of the electroactive analyte, or mediator, takes place [77]. Significant applications of voltammetric sensors comprise the detection of small and biorelevant organic molecules essential to monitor the health of the human system (e.g., dopamine, ascorbic acid and uric acid) [73,78]. On the contrary, amperometric measurements are performed at a constant potential. The Faradaic current, generated during the redox reactions of the electroactive molecule, is recorded continuously and used to determine the concentration of the analyte. 2D materials have been used to design amperometric sensors applied in the fields of health, environmental, food, and

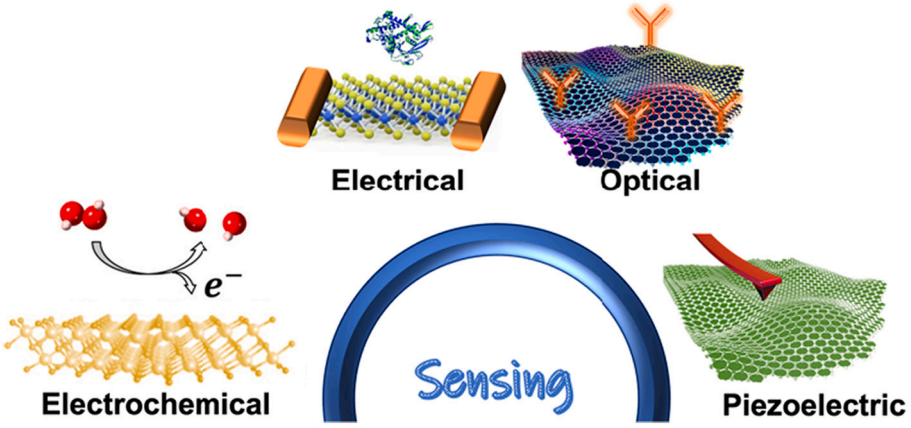

Fig. 4. Transduction mechanisms for 2D materials in sensing: electrochemical, electrical, piezoelectric and optical.

agriculture monitoring [79].

3.2. Electrical mechanism

Among the several electrical sensors using 2D materials, field-effect transistors (FETs) are the most promising as they can provide elevated sensibility, robustness, fast detection and easy operability [80,81]. Generally, FETs use the 2D material as a transport channel, driving charges injected from the electrode and accumulated in the semiconductor thanks to their elevated electrons and hole mobility. In fact, FETs present ambipolar performance, which involves the conduction of positive and negative species. When 2D materials are exposed to different species, a charge transfer mechanism occurs between the semiconductive materials and the adsorbed molecules. This interaction results in different changes in resistance [82]. Moreover, FETs are highly sensitive, reliable, low-energy consuming and have a reduced recovering time compared to chemiresistor devices [83]. FETs and electrical sensors based on 2D materials have been proposed as proof-of-concept devices with applications in mechanical, optical, gas, ion, protein and bioelectric sensing [84].

Another electrical transduction principle relies on conductometric measurements. Conductimetric sensors take advantage of the ability of some analytes to modify the electrical current flowing between two electrodes. In this field, 2D materials, specifically 2D hybrid nanomaterials including layered TMDs, graphene [85], and BP [86], play a pivotal role in gas sensing at room temperature. These materials demonstrated fascinating performances due to the large surface area, high number of active sites, room-temperature conductivity and tunable optical properties.

3.3. Piezoelectric mechanism

Piezoelectric sensors are physical sensors with high sensitivity that have been applied in a wide number of applications. When stress is applied, the resistance of piezoelectric sensors changes depending on geometric factors and the resistivity effect. The resistance of a semiconductor under tension can be expressed as a function of the resistivity, length and average cross-sectional area. The gauge factor (GF) is popularly used to evaluate the sensitivity of strain sensors, which convert external stimuli into electrical signals. Sensitivity can also be expressed as the ratio between the change in normalized resistance and the applied strain.

Graphene has been widely employed in piezoelectric sensors due to its inherent piezo-electrical properties, such as the linear change of resistance in the function of the strain. In particular, graphene piezoresistivity is attributed to three mechanisms: (a) structural deformation, (b) over-connection of graphene sheets, and (c) the tunnelling effect among neighbouring sheets [87]. However, aside from graphene, in-plane and vertical piezoelectricity have been predicted and demonstrated for TMDs (d33). However, the challenge of controlled synthesis of TMDs with large size (centimetres scale), high crystallinity and good reproducibility limits their application in large-area integrated, flexible sensor arrays [88]. It is worth mentioning that there are many examples of piezoelectric sensors in which graphene is introduced in 3D structures: 3D scaffolds, microstructures with polymers or (micro)fibers [89]. However, this review only collected 2D-material-based examples.

3.4. Optical mechanism

Optical sensors are typically simple and cost-effective devices able to quantify different properties of light, such as intensity, wavelength, frequency, polarization and scattering. Optical techniques present advantages compared to electrical sensors since they are not affected by electromagnetic interferences, possess chemical inertness, and allow remote sensing. Furthermore, optical sensors can be highly sensitive and even capable of single-molecule detection. On the other hand, the combination of unique optical properties, high conductivity, exceptional electron mobility, and the large surface-to-volume ratio of the presented 2D materials have become the ideal platform for creating optical sensors [90]. Moreover, dopants or metallic nanostructures could assist in the enhancement of the targeted signal [64,91]. Overall, the application of optical sensors based on 2D materials is rapidly growing in many essential fields such as biomedicine, environmental monitoring, and food analysis [92].

In this section, we review the dominant technologies used to transduce light signals in optical sensors: surface plasmon resonance (SPR), surface-enhanced Raman spectroscopy (SERS), and fluorescence resonance energy transfer (FRET) [90,92].

3.4.1. Surface plasmon resonance

Plasmonic sensors have been exponentially growing in the fields of biochemical and environmental monitoring. In principle, plasmonic sensors are based on the surface plasmon resonance methodology, which is produced by the oscillations of conduction electron density and the electromagnetic wave on a material surface under a specific stimulus such as photons, electrons and phonons [93]. Some of the 2D materials described here as graphene and TMDs are widely used for SPR sensing due to their attractive physicochemical properties [94]. However, few researchers have directly utilized the plasmonic effect of 2D materials in the fabrication of SPR sensors [94,95]. In fact, the low absorption of 2D nanomaterials in the visible and NIR range of the spectrum has limited their direct application in plasmonic sensors. Thus, instead of 2D nanomaterials, Au or Ag are frequently used to enhance the performance of plasmonic sensors

3.4.2. Surface-enhanced Raman spectroscopy

Raman spectroscopy is a common non-destructive analytical technique which enables the structural identification of molecules as a fingerprint. The application of Raman scattering in sensing is often restricted due to the feeble signals that can be collected at a low analyte concentration. SERS, discovered by Fleischmann *et al.* in 1974, has attracted extensive interest for its ultrasensitive detection of multifold analyte traces (*i.e.*, enhanced up to 10^{10}) [96,97]. The mechanisms behind SERS are based on two phenomena: electromagnetic enhancement (EM) and chemical enhancement (CM). In detail, EM is originated from the localized surface plasmon resonance (LSPR), and CM arises from the charge transfer due to dipole-dipole interactions between the analyte and the substrate [98].

2D materials serve as efficient substrates for SERS due to their low cost, easy synthesis, outstanding optical properties, and good biocompatibility [99]. For these reasons, 2D materials provide an interesting alternative to noble metals, the state-of-the-art materials in SERS. In fact, noble metal, even if highly efficient, presents a series of drawbacks such as high cost, strong metal-adsorbate interaction, reduced stability in time, and catalytic and photobleaching effects [97]. A popular strategy is to combine 2D materials with noble metals, creating nanocomposites able to overcome the drawbacks of both.

3.4.3. Fluorescence resonance energy transfer

Fluorescence sensors present elevated sensitivity, straightforward and low-cost design strategies, and portability [100]. Due to their photoluminescent properties, the 2D materials described in this review can be used in fluorescence-based chemical sensors as a quencher or fluorophore [101]. In this section, we discuss the mechanism of how 2D materials sensors operate through the fluorescence resonance energy transfer (FRET) process.

FRET is considered a non-radiative energy transfer process having a fluorescent donor and a light-absorbing acceptor. This phenomenon takes place when the emission spectra of the donor and the absorption spectra of the acceptor overlap (<10 nm) [102]. Generally, 2D materials present a good quenching capability [103]. Similarly, TMDs [103–105], have been employed as acceptors in FRET sensors in diverse fields, including cellular imaging, single molecule spectroscopy, biochemical analysis and environmental monitoring [106].

4. Sensing applications

In this section, we reviewed the advances of 2D materials in the field of sensing. Along the following pages, we collected several examples of sensing based on 2D materials in the areas we consider needing to be updated, involving physical, chemical, and wearable sensors. Further comparative details and examples of this section can be found in Table 1.

4.1. Physical and chemical sensors

The working principle of physical sensors resides in the transduction of changes in physical properties of the matter into electroresistive optical or mechanical outputs. These changes depend on morphological characteristics such as single or multi-layer, intercalation species and externally switched potential bias [107,108]. On the other hand, the identification and quantification of chemical species is a topic of paramount importance. The monitoring and ultra-sensitive detection of these compounds has been deeply studied, founding several applications in the fields of environmental protection, safety, or clinical diagnosis [109]. The performance of a chemical sensor based on 2D materials is very similar to other approaches described above, the surface of the material is able to sense a chemical specie, and the analytes interact with the surface of the bidimensional material. In some cases, chemical functionalization, natural defects, and/or doping of the surface of 2D

Table 1
Additional information of 2D Materials towards sensing technology.

Material	Tuning approach[a]	Mechanism	Target	Limit of detention	Sensitivity	Reference
MXene/Prussian blue ($Ti_3C_2T_x$)	NC	Electrochemical	Glucose and Lactate	$0.33\bullet10^{-6}$ M $0.67\bullet10^{-6}$ M	35.3 μA mm^{-1} cm^{-2} 11.4 μA mm^{-1} cm^{-2}	[176]
MXene/PVA hydrogel ($Ti_3C_2T_x$)	NC	Electrochemical	Facial expression	-	25 (GF)	[208]
Mxene/PDMS (Ti_3C_2)	NC	Piezoelectric	Human motion	-	7400 (GF)	[194]
Mxene ($Ti_3C_2T_x$)	N.A.	Electrical	VOC	50 ppb	<ppm	[137]
Mxene/PVA ($Ti_3C_2T_x$)	NC	Electrical	VOC	50 ppb	0.10 ppm^{-1}	[138]
AuNPs/Mxene-PDDA ($Ti_3C_2T_x$)	NC	Electrochemical	Nitrite	0.059 μM	250 μA mM^{-1} cm^{-2}	[209]
Mxene (Ti_3C_2)	N.A.	Optical	Hg^{2+}	42.5pM	0.05-50 mM	[210]
Mxene ($Ti_3C_2T_x$)	N.A.	Optical	Ag	0.615 μM	-	[145]
Graphene-Pyrene	NC	Electrical	Interferon Interleukin tumor necrosis factor	$476\bullet10^{-15}$M $608\bullet10^{-15}$M $611\bullet10^{-15}$ M	-	[180]
Graphene	N.A.	Electrical	Brain stimulation	116.07–174.10 μC cm^{-2}	-	[192]
Graphene-MoS_2	NC	Piezoelectric	Human Motion		6.06 kPa^{-1}	[211]
rGO	N.A.	Piezoelectric	Human motion	-	25.1 kPa^{-1}	[198]
rGO/cellulose fibers	NC	Piezoelectric	Human motion	8 μm	−8.9 (GF)	[197]
Carboxyphenyl-G	C	Electrochemical	Ovalbumin	0.9 pg mL^{-1}	-	[69]
rGO-aryl fluoride	C	Electrochemical	Ammonia	20 ppm	63%	[70]
rGO-ferrocenylaniline	C	Electrochemical	Tumor necrosis factor	0.1 pg mL^{-1}	-	[71]
Pt-loaded/h-BN	NC	Electrical	Propane	2%	20000 ppm	[212]
h-BN	N.A.	Electrical	NO_2	20 ppb	1.645 ppm^{-1}	[51]
$MoTe_2$	N.A.	Electrical	Ketone	0.2 ppm	100 ppm	[27]
WS_2	N.A.	Electrical	NH_3	1 ppm	10 ppm	[119]
MoS_2	N.A.	Electrical	Pressure and temperature		~51 kΩ °C^{-1}	[213]
MoS_2/hBN	NC	Electrical	NO_X	6 ppb	6 ppb	[214]
MoS_2	N.A.	Electrical	NO_2	0.15 ppb	1 ppb	[132]
MoS_2	N.A.	Optical	Methanol	2.7 ppm	-	[215]
MoS_2/Au	NC	Optical	Antigen	0.5 pg/mL	-	[216]
MoS_2/rGO	NC	Electrochemical	H_2O_2	0.19 μM	101.70 μA mM^{-1} cm^{-2}	[217]
MoS_2/rGO	NC	Electrochemical	NO_2	0.17 μM	0.46 μA μM^{-1} cm^{-2}	[133]
BP/PEI-PEG	NC	Flexible	CO_2	200 ppm	-	[218]
BP	NC	Electrical	NO_2	20 ppb	20% for 20 ppb	[42]
BP	N.A.	Electrical	NO_2	5 ppb	5 ppb	[43]
BP	N.A.	Electrical	NH_3	80 ppb	10 ppm	[44]
BP-AuNPs	NC	Electrochemical	Patulin	0.03×10^{-3}M,	–	[219]

[a] NC (Non-covalent), C (covalent), N.A. (not applicable).

materials could improve the sensitivity and trapping of detected chemical species.

4.1.1. Electroresistivity

Gas sensing is the most extended application of 2D materials referred to electroresistivity, and it can be divided into two main categories: chemiresistor and FETs [64]. Their work-principle are underpinned by the changes detected during the adsorption of a gaseous analyte, *i.e.* resistance for chemiresistor and drain current for FETs. This interaction is weak with bare 2D material and gaseous analyte, but it can be engineered depending on the chemical composition of the material used. For example, MXene possesses terminal oxygen groups, and g-CN includes amines on its surface, allowing essential chemical modifications and hydrogen-bonding interactions. Other 2D materials, such as BP or h-BN nanosheets, present limitations due to their reduced light and oxygen stability [107]. The most common gas-sensing analytes include hydrogen (H_2), ammonia (NH_3), nitrogen oxides (NO_x), and sulfur dioxide (SO_2). Frequently, reports of gas sensors are combined with theoretical calculations where the interactions between the gaseous analyte and the pristine material are explained [64]. Even though TMDs present low sensitivity toward nonpolar molecules, dopant incorporation (generally metals) alters the electronic structures of the materials and improves the sensor capability [64].

4.1.1.1. FETS. Feng *et al.* studied NH_3 and NO_2 sensing properties of molybdenum telluride ($MoTe_2$) using FET based on this material and found it extremely sensitive to these gases. They demonstrated that the recovery kinetics could be effectively adjusted by biasing the sensor to different gate voltages, achieving 90% recovery after each sensing cycle within 10 min at room temperature. They also presented a sensitive detection of NO_2 and NH_3 with low detection limits of 12 ppb and 1 ppm, respectively [110]. FETs made by Tungsten Disulfide (WS_2) exfoliated nanoflakes were used for ethanol and NH_3 sensing. The FET showed high electron mobility of 12 $cm^2 \cdot V^{-1} \cdot s^{-1}$ and response in the presence of reducing gases, thanks to its n-type nature. On the contrary, the material presented significant drawbacks in the presence of oxidizing gas such as oxygen, which depleted its n-type behavior, reducing the conductivity [111]. Molybdenum diselenide ($MoSe_2$) multilayer synthesized by CVD was used to manufacture FET for NO_2 gas sensors with ultra-high sensitivity (300 ppm), real-time response, and rapid on-off switching. The device showed n-type behavior with field-effect mobility of 65.6 $cm^2 \cdot V^{-1} \cdot s^{-1}$. The hole current significantly increases when it is exposed to NO_2 gas, which is attributed to extra band gap states induced by the absorbed NO_2 gas [112]. In other examples where $MoSe_2$ was gold-assisted exfoliated and deposited within a flexible substrate (see Fig. 5a), the FETs device presented selectivity for detectingNO_2 and NH_3 in the ranges of 2-10 ppm and 5-25 ppm, respectively (Fig. 5b). The nanocomposite exhibited excellent n-type electrical properties, including a high on/off ratio (>106), high mobility (42.6 $cm^2 \cdot V^{-1} \cdot s^{-1}$ for monolayer) and low threshold voltage (−8 V). In this soft device, FET was displayed on human skin and connected to a flexible print circuit board (PCB) configuration for streaming and wireless recording (see Fig. 5c-d) [113]. Additional, Hong *et al.* used polydimethylsiloxane (PDMS) stamp to transfer tungsten diselenide (WSe_2) flake from its bulk counterpart to fabricate a back-gated p-channel FET for detection of various oxidizing and reducing gases at room temperature. Thus, when the device was exposed to equal concentration (1 ppm) of four different analytes (*i.e.*, NO_2, SO_2, NH_3, and H_2S) the maximum response was obtained for NO_2 while the minimum response was recorded for SO_2 [114]. Exfoliated MoS_2 nanoflakes,

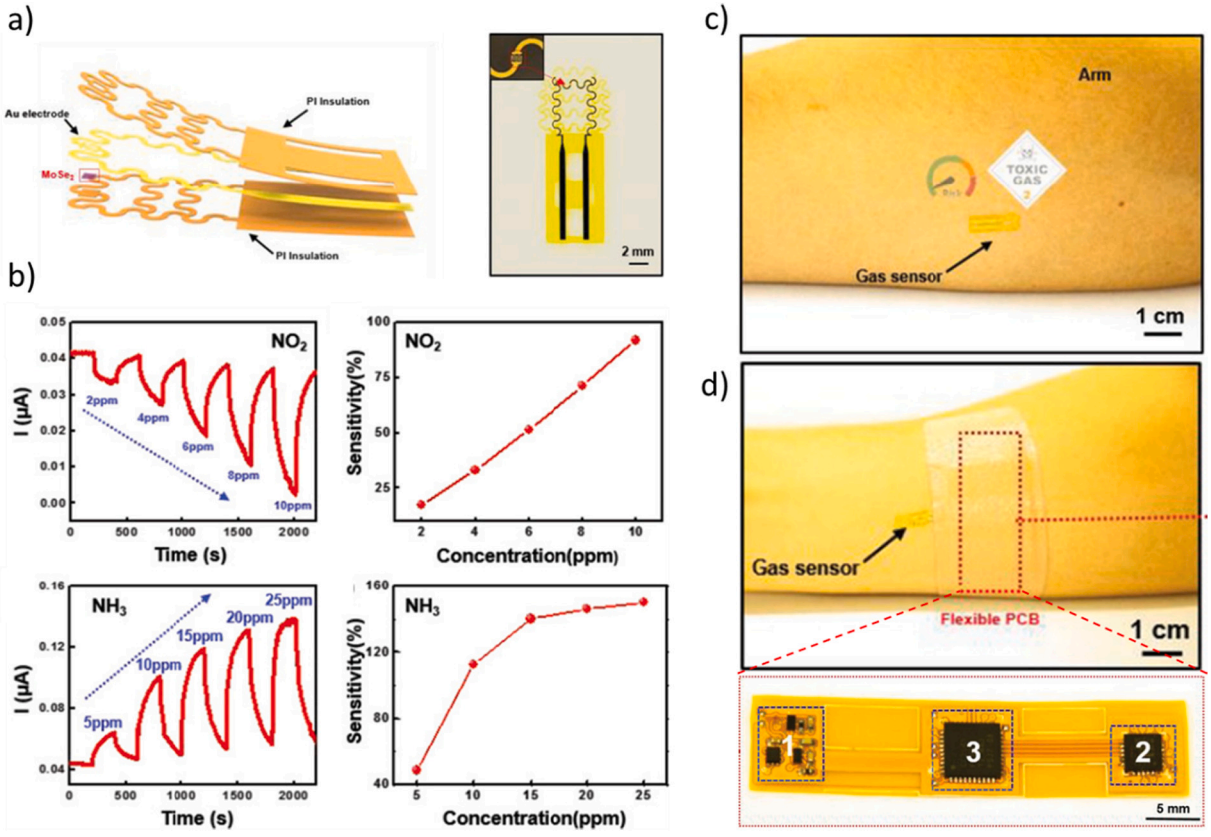

Fig. 5. a) 3D Scheme of the device deposited on the gold structure and encapsulated on a flexible substrate, b) Response (left) and sensitivity (right) curve to different concentrations of NO_2 and NH_3 (V= 5 V), c) Patch on relaxed human skin to test and record gas data. d) Optical image of the assembly of the device with flexible PCB under the bandage, and optical image of detailed block circuit on flexible PCB, where 1 is the voltage divider part, 2 is the amplifier, and 3 is the microcontroller. (Figure adapted from reference [113])

annealed in air either at 150 °C or at 250 °C, produced ambipolar behavior with NO_2 sensing capabilities. The sensor, annealed at 150 °C in air, exhibited p-type behavior under NO_2 analyte. This behavior is potentially ascribed to nitrogen substitutional doping of S vacancies in the MoS_2 surface. Meanwhile, annealing at 250 °C resulted in n-type behavior with 20 ppb sensitivity to NO_2 and a response as high as 5.8 times for low concentration of NO_2. As well as NO_2, n-type showed good electrical response under H_2 [115].

4.1.2. Chemiresistive

In a pioneer study, Zhou *et al.* studied the specific interaction of toxic gas molecules (H_2, O_2, NH_3, NO, NO_2, and CO) at the surface of WS_2 monolayers by density functional theory (DFT). Band structure calculations showed that the valence and conduction bands of monolayer WS_2 are not disturbed upon adsorption of H_2, NH_3, and CO. However, some of the lowest unoccupied orbitals for O_2, NO, and NO_2 are pinned around the Fermi-level when they are adsorbed on the monolayer of WS_2 [116]. Apart from NO_2, n- and p-type WS_2 materials were used by several authors for proton-rich analytes such as ammonia and water. Some authors suggested the effect of an increase in acidity when adsorption and/or solvation-assisted of these molecules were onto the surface of the material, producing a catalytic effect [108].

There are a large number of examples for chemiresistive 2D material sensors. For instance, Matatagui and co-workers developed a very easy, low-cost, on-paper substrate WS_2 nanoplatelets device by abrasion-induced deposition. The device was employed successfully for high-sensitivity and selective detection of NO_2 at room temperature [117]. WS_2 nanosheets fabricated by liquid exfoliation were deposited by drop casting on interdigitated electrodes (IDE) and used as chemiresistive humidity sensor. The affinity to protons indicated an n-type performance of the exfoliated WS_2. The response of the sensor varied from 11.9 to 80% relative humidity (RH). The sensor exhibits swift response-recovery characteristics when exposed to different RH levels. The corresponding response time was found between 13s (11.9% RH) and 17s (80% RH) [118]. In another work, Li *et al.* ball milled commercial bulk WS_2 powder to obtain p-type WS_2 nanoflake. In this case, IDE with 200 μm gap electrodes was prepared by dip coating. The sensor performance indicates good sensitivity and response/recovery speeds to the different concentrations of ammonia from 1 to 10 ppm at room temperature [119].

Apart from exfoliation methods, there are other works that grow the material "*in situ*" on top of the device. O'Brien *et al.* presented a method for low-temperature synthesis of WS_2 throughout the sulfurization of tungsten trioxide (WO_3) using H_2S plasma. Interdigitated WS_2 electrodes were manufactured with WO_3 sputter dependence thickness. A sensitivity of 1.4 ppm NH_3 in nitrogen at room temperature was achieved [120]. As interesting as CVD, ultra-thin WS_2 nanosheets with a thickness of about 5 nm were synthesized by an economical hydrothermal method combined with a calcination process. Three-dimensional wall-like structure was formed by the interconnecting WS_2 nanosheets. The resistive gas sensors achieved a superior response of 9.3% to 0.1 ppm NO_2 gas at 25 °C and good stability in low and moderate humidity [121].

Regarding WSe_2, Guo *et al.* reported a simple and effective method to exfoliate WSe_2 into few-layered nanosheets with N-methyl-2-pyrrolidone (NMP) as a dispersant. The chemiresistive sensor showed excellent selectivity, extremely high response (50 ppb) under a low detection concentration of NO_2 and reliable long-term stability within 8 weeks. The authors hypothesized a mechanism based on the physisorption of the NO_2 gas molecules and charge transfer between the surface of WSe_2 nanosheets and the molecules of NO_2 adsorbed. The electrophilic NO_2 molecules on the surface of WSe_2 nanosheets extract electrons from the valence band of WSe_2, increasing the hole concentration and reducing the resistivity of the sensor [122].

On the other hand, a monolayer of MoS_2 was selected as a chemical sensor with high selectivity for trimethylamine (TEA). The response mechanism refers to the transient surface physisorption that affects the conductance of the MoS_2 monolayer. The authors compared TEA sensing against conventional carbon nanotubes-based gas sensors. Interestingly, MoS_2-based devices showed a high order of selectivity compared to the tube-based device [123].

Cho *et al.* grew by CVD layered-MoS_2 using molybdenum trioxide (MoO_3) and a sulphur powder as a precursor. They deposited the material onto a sapphire substrate forming interdigitated electrodes with 100 μm of separation (see Fig. 6a). Transient resistance responses were investigated in two analytes gases, NO_2 and NH_3, at concentrations from 1.2 to 50 ppm. In the NO_2 gas mode, the resistance increased at room temperature and 100°C (positive sensitivity). In this case, NO_2 acted as an electron acceptor, bringing the Fermi level closer to the valence-band edge and resulting in p-doping. Meanwhile, NH_3 acted as an electron donor (*i.e.*, n-doping), shifting the Fermi level of the MoS_2 to the conduction-band edge; therefore, it possesses a negative sensitivity at both temperature regimens (see Fig. 6b). The surface of the material was saturated at approximately 20 ppm, irrespective of the operating temperature, as observed in Fig. 6c. Finally, the authors also confirmed by DFT the charge-transfer mechanism between the gas molecules and the MoS_2, besides its probabilistic position within the mechanism proposed (see Fig. 6d) [124].

A simple but effective method for fabricating large-scale TMDs layers on a flexible substrate was reported by Zhao and coworkers. MoS_2 was grown at a low temperature of 200 °C directly on hard (SiO_2) and soft substrates (polyimide, PI) *via* CVD with molybdenum carbonyl ($Mo(CO)_6$) and H_2S. The grown crystal produced by low temperature possesses a layered structure with good uniformity, stoichiometry, and a controllable number of layers, characterized by Raman spectroscopy. MoS_2 grown on a soft substrate was used to sense ammonia and NO_2. By applying 500 ppm of an analyte, the 2D MoS_2-based flexible gas sensor showed a much higher NO_2 response of approximately 300% compared with the NH_3 response of approximately ~ 5%. The difference resides in the adsorption of the gas molecules on the defect or basal plane due to the 2D nature. The sensing was also performed with a bending radius of ~7 mm, and the durability of the MoS_2-based flexible gas sensor was evaluated upon 2000, 4000, and 6000 bending cycles [125]. Cho *et al.* used a CVD approach based on a controlled vertical and horizontal growth of the MoS_2 nanosheets, boosting the sensing capabilities of the material throughout the area exposed. They compared different electrode configurations of MoS_2 nanosheets exposure for NO_2 sensing capabilities: basal plane (horizontal), edge (vertical) and a mixture of basal plane/edge exposed (horizontal and vertical). They found fivefold enhanced sensitivity when edge exposed configuration was used and demonstrated its area-in-contact dependence [126]. In the line of nanoshapes, cone-shaped (CS)-MoS_2 bilayers were grown by depositing 2 nm-thick MoO_3 layers on a 2″ three-dimensional (3D) cone-patterned sapphire substrate (CPSS) followed by a sulfurization process *via* chemical vapor deposition. The sensor was used for ppb level detection of NO with a large response (200%). This architecture improved the sensing at room-temperature thanks to the increase up to 30% of the exposed area [127].

Single- and few layers of $MoSe_2$ nanosheets were deposited at room temperature by mechanically exfoliating bulk crystals onto pre-cleaned 300 nm SiO_2/Si substrates. The as-prepared $MoSe_2$ gas sensor devices were fabricated using electron-beam lithography and presented a non-linear response for ammonia concentrations ranging from 50–500 ppm [128]. $MoSe_2$ chemiresistive devices were synthesized *via* ultrasonication-assisted liquid exfoliation in other work. The size of the nanoflakes was tuned by varying the centrifugation speed. Moreover, the exfoliated material was drop casting in an interdigitated electrode and used as a sensor for selective H_2S gas at 200°C. The response of the device was driven between 15.87–53.04 % for H_2S concentration of 50 ppb–5.45 ppm when operated in ambient and 7.13–19.87 % for the concentration range of 500 ppb–5.45 ppm when performed in a flowing environment of synthetic air [129].

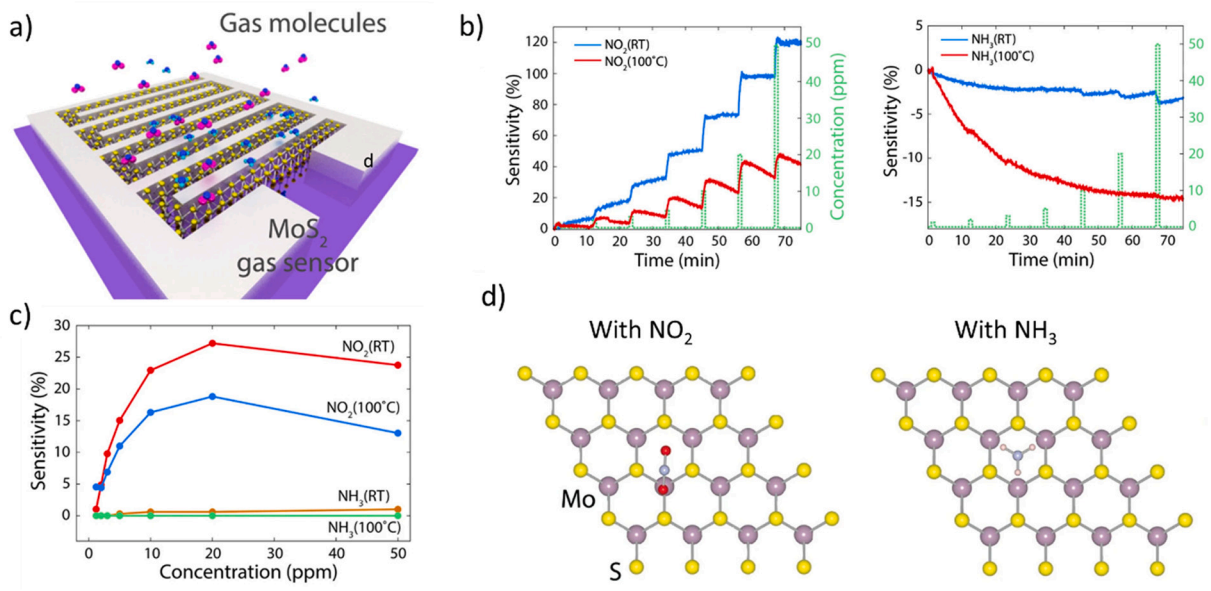

Fig. 6. a) 3D schematic of the interdigitated electrode of MoS_2 on sapphire, b) Transient cure for NO_2 (left) and NH_3 (right) gas response from 1.5 to 50 ppm gas, operating at room temperature and 100°C. In the NO_2 gas mode, the resistance increases (positive sensitivity). c) Sensitivity comparison of NO_2 and NH_3 gases at different gas concentrations and operating temperature and d) top views of the most favorable configurations for NO_2 (left) and NH_3 (right) on the MoS_2 (figure adapted from reference [124]).

Choi *et al.* reported a $MoSe_2$ nanomaterial doped with niobium (Nb) for NO_2 gas sensor. Nb was carefully incorporated *via* plasma and compared with pristine $MoSe_2$. Control of the doping was demonstrated for optimum gas sensing response. In the first round of doping ($MoSe_2$: Nb-1C), the sensor yielded the highest response for detecting 3 ppm of NO_2. They hypothesized that incorporating Nb increased the surface area to volume ratio, making it more sensitive than pristine $MoSe_2$. However, the increment of Nb dopants caused a significant increase in the number of metallic niobium diselenide ($NbSe_2$) clusters, which were not responsive to gaseous molecules, dropping the effectiveness of the sensor [130].

In a new addition to the class of layered TMDs, $MoTe_2$, Zhang and coworkers used the typically great chemisorption of TMDs for NO_2, combined with its photoresponsivity properties that enhance the recovery rate of the sensor. The exfoliated material increases the sensitivity by one order of magnitude under 254 nm UV illumination compared to dark conditions, leading to a meagre detection limit of 252 ppt. Furthermore, the recovery rate was improved from 10% to 40% in dark conditions to 100% under UV illumination within 160 s at different NO_2 concentration ranges. Finally, the p-type $MoTe_2$ sensor also exhibited excellent sensing performance to NO_2 in ambient air, indicating its great potential in practical applications [131]. Using analogous approaches with TMDs similar behaviors were observed [132,133].

On the other hand, Gautam *et al.* have synthesized a tridimensional architecture of h-BN for humidity and liquefied petroleum gas (LPG) detection. They used a bottom-up approach using a mixture of boron trioxide (B_2O_3) and h-BN. Afterwards, the as-prepared material presented a tridimensional porous architecture. Similar to other 2D materials, the method for sensing within the prepared material was based on chemisorption. In this example, the h-BN showed a resistivity range from 1.47 to 0.29 MΩ/%RH for low (10–40% RH) and for high (40–90% RH) humidity, respectively [134,135]. Using a low-temperature solvothermal method to synthesize h-BN, the material showed a nearly transparent morphology with a thickness of ~1.36 nm (four atomic layers). The variation in conductance was caused by charge transfer between the chemical absorption/desorption process of oxygen molecules on the sensor surface. The gas sensed 100 ppm at different working temperatures. In detail, ethanol sensitivity reaches 1.72, 2.9 and 4.5 by increasing the temperature to 240, 260 and 300 °C. Moreover, the device presented a fast recovery along the time and good response ability [136].

The good conductivity of MXenes, as well as a large number of functional groups on their surface, makes them good candidates for chemical sensors, unlike other materials such as pristine graphene (often with an inert surface and a weak uptake of chemical species) or MoS_2 (with high selectivity performances but lower signal to noise ratio).

The relevance of which elements are found on the surface of the device is demonstrated by Kim and co-workers [137]. They developed a MXene chemical sensor with high selectivity to detect volatile organic compounds (VOC). The good LOD of the sensor is caused by the conductivity of the material. Besides, the surface, enriched by various functional groups, contributes to the selectivity and good interaction of the VOC. The authors test one type of MXene (Ti_3C_2Tx) and highlight the potential possibilities for improvement due to the rich diversity of this family of compounds. Excellent results have also been obtained by Yuan and co-workers in the self-assembling of the MXene by electrospinning. The sensors showed good versatility and flexibility with no decrease in performance after 1000 cycles, demonstrating great potential for industrial applications [138].

4.1.3. Optical-based sensing

4.1.3.1. Raman spectroscopy sensor. Lu *et al.* reported a device based on graphene oxide (GO) decorated with Ag nanoparticles (AgNPs) for detectioning nitroaromatic compounds by surface-enhanced Raman scattering. In detail, different fluorophores such as rhodamine 6G, methyl violet and methylene blue were detected. The device performed with sharp and intense peaks when the GO-AgNP combination was used. The results showed some order of magnitudes of improvement than pristine GO. These results suggested the crucial role of the AgNP in enhancing the signal [139]. Gold nanorods (AuNR) stabilized with poly (N-vinyl-2-pyrrolidone) were self-assembled with GO *via* electrostatic interactions. The GO–AuNR materials showed a great increase of the Raman signal for the detection of crystal violet and neutral red aromatic dyes, which demonstrated the use of cationic and anionic aromatic dyes as molecular probes [140].

Criado and co-workers proposed an exfoliation method that leads to

highly-enriched 1T phase MoS_2 (94.5%). The exfoliated 1T-MoS_2 showed surface-enhanced Raman scattering with a low detection limit throughout rhodamine 6G and crystal violet [34]. The same material but modified with a monoclonal antibody was used as a capture probe of α-fetoprotein (AFP) at highly detection level (1 pg mL^{-1} to 10 ng mL^{-1}) and LOD lower than 0.03 pg·mL^{-1}. They decorated the functionalized MoS_2 with silver-coated gold nanocubes to increase the density of "hot spots" on the surface of the immunosensor [141]. Similarly, Su *et al.* decorated MoS_2 nanosheets with gold nanoparticles to detect rhodamine 6G. The mixture of both materials produced an amplification of the signal in comparison with the pristine itself. They also observed the necessity of control and precision of the functionalization for a maxima optical signal. The SERS enhancement capacity was therefore associated with particle aggregation, where the number of hotspots was maximized [142]. Aside from TMDs, Ti_3C_2 functionalized decorated with silver, gold or platinum nanoparticles was synthesized to detect methylene blue throughout surface-enhanced Raman scattering. As well as in the other TMDs, the functionalized 2D material showed an enhancement of the analyte signal besides slight shifts in peak positions. The authors determined the enhancement factors based on the nanoparticles-decorated Ti_3C_2, *i.e.*, silver, gold and palladium, to be $1.50{\cdot}10^5$, $1.17{\cdot}10^5$ and $9.61{\cdot}10^4$, respectively [143].

4.1.3.2. Colorimetric sensors. Metal ions can be easily detected by colorimetric assays based on 2D material sensing platforms. Zhang *et al.* performed a colorimetric detection of Hg^{2+} in aqueous solutions mimicking peroxidase performance. Two-dimensional rGO/PEI/Pd nanohybrid was synthesized for such purpose. The presence of mercury ions makes the nanohybrids rGO/PEI/Pd promoted oxidation, and 3,3′,5,5′-tetramethylbenzidine (TMB) produced from dark to blue color that could be detected by the naked eye. The nanohybrids performed an ultralow detection limit of 0.39 nM for Hg^{2+} in ddH_2O and ~1 nM in wastewater [144].

Wang and coworkers showed an easy procedure using MXenes as a trigger of optical signals through the reduction of Ag^+ to Ag NPs. These NPs remain on the surface of the material, having good selectivity. Besides its detection on a UV-vis spectrometer, the authors report the possibility of detecting it through a conventional smartphone [145].

4.1.4. Flexible photodetectors

Apart from conventional sensors, 2D materials have been reported as highly efficient channel materials in photodetectors. TMD-based photodetectors exhibit broad spectral detection, short response time, low dark current, high responsivity, and tunable electrical properties [88].

The 2D InSe material was manufactured on flexible polyethylene terephthalate (PET) photodetectors or rigid on SiO_2/Si substrate. The InSe presented a broad-band ranging from the visible to near-infrared regions (450–785 nm), high photoresponsivities up to 12.3 A·W^{-1} at 450 nm (on SiO_2/Si) and 3.9 A·W^{-1} at 633 nm (on PET). Besides, the photodetector possesses a response time of ~50 ms and exhibits long-term stability in photoswitching [146]. Castellanos and co-workers presented an easy-to-implement technique in which large-area WS_2 photodetectors were manufactured on top of flexible polycarbonate substrates. WS_2 photodetector on polycarbonate presented well-balanced performances with responsivity up to 144 mA·W^{-1} at 10 V of V_{sd}. The photodetector response time was down to ~70 μs with a detective value of 10^8 Jones [147]. The electrode was fabricated using an abrasion-induced method previously reported. This powerful technique was illustrated by manufacturing 39 different Van der Waals materials on standard copy paper, including superconductors, semi-metals, semiconductors, and insulators [148]. Few layers of $MoSe_2$ films were modified with amine-terminated poly(styrene) to form a p-n junction photodetector. The device shows a fast response time of 100 ms, a responsivity of 2.5 A·W^{-1} and a high detectivity value of $2.34{\cdot}10^{14}$ J. The device was flexible and stable after 1,000 bending cycles, *i.e.* curvature of 7.2 mm [149].

4.1.5. Flexible Piezo-resistivity sensors

CVD graphene synthesized onto SiO_2 was first photolithographed and then treated with reactive ion-etching to manufacture a device in a desired shape and dimension. After that, 2 mm thickness of polydimethylsiloxane (PDMS) was transferred onto the patterned graphene. The final instrument was a transparent and stretchable strain sensor. The strain sensor had a GF between 2.4 and 14. The lower GF was similar to traditional metallic strain gauge materials [150]. In other work, PDMS was modified and transferred on top of a ripple-like morphology with a certain periodicity. The manufactured sensor was used as strain-based sensor and presented a strong dependence on their original shapes and ripple-dependence morphology. The rippled graphene could afford large strain deformation while giving a negative GF (-2) when the applied strain was performed from 0-20%. On the opposite, the buckled graphene showed high GF values when increased from 0 to 30% due to the re-arrangement of graphene domains [151].

In the way of using other polymers as a flexible substrate, polypropylene was coated with graphene solution by the layer-to-layer method. The device showed excellent durability and a high GF (~1000) in the strain range of 0.05% to 0.265%. Moreover, it was used for the detection of wrist pulse, finger bending and throat movement during pronunciation [152]. rGO doped with polystyrene nanoparticles was assembled to manufacture a highly responsive, flexible piezoresistive strain sensor. The sensor was prepared by depositing a mixed solution of PS nanoparticles and GO fragments onto PDMS film, followed by laser-scribe patterning through thermal reduction (see Fig. 7a). The work-function of the sensor consisted of a change in the physical stacking of rGO fragments, producing a deformation. It creates partially connected conducting channels that can amplify the signal as resistance changes. Accordingly, even under minor strains of 1.05%, GF values of 250 could be obtained. The device was used for real-time monitoring of human body activities, including swallowing, lower back posture and pulse on the neck. Fig. 7b shows the increasing and decreasing of the resistance associated with the pharyngeal phase and esophageal phase, as the result of larynx and pharynx movements and muscle stress. In Fig. 7c, the sensor was attached to a human's lower back to monitor different back bending postures (form P1 to P4). Since resistance change is related to strain deformation, the differences can be used to evaluate the level of muscle tension [153].

Across the synthesis of ultra-long CVD graphene bundles, Wang *et al.* fabricated core−sheath nanofibers significant valuable for flexible and wearable microelectronics. First, the graphene wires were grown on dozens of copper wires (~80 wires) by the CVD method. After copper wires etching, they coated it again with different concentrations of Polyvinyl alcohol (PVA), forming G@PVA core−sheath fibers with various sheath thicknesses. The highest concentration of PVA (G@10wt %) presented a mechanical strength of 590 MPa, besides a high conductivity of $9.6{\cdot}10^3$ S·m^{-1}. The fiber exhibited a highly sensitive response to the bending and stretching forces in terms of relative resistance change [154]. In other work related to wires, silver nanowires and graphene were embedded in a polyurethane matrix forming a film and used as a composite for physical vibrations, wrist pulses and recognition of sound. The composite presented a GF high as 20 for strain changes less than 0.3%, 1000 in the $0.3\% < \Delta\varepsilon < 0.5\%$ range, and 4000 in the $0.8\% < \Delta\varepsilon < 1\%$ strain range. This strain gauge also displayed high sensitivity to bending, high strain resolution and high operating stability [155]

Referring to TMDs, an ultrathin conformal MoS_2-based device was integrated with a graphene electrode to result in a flexible tactile sensor. The sensor shows high sensitivity, good uniformity, and linearity even after 10,000 loading cycles. Moreover, the device worked over a strain of 1.98% and had good optical transparency of over 80%. The MoS_2/graphene flexible electrode was used as a high-density array electrode and high switching speed through active matrix circuitry [156]. MoS_2, situated within dielectric sandwich layers, was engineered to achieve a

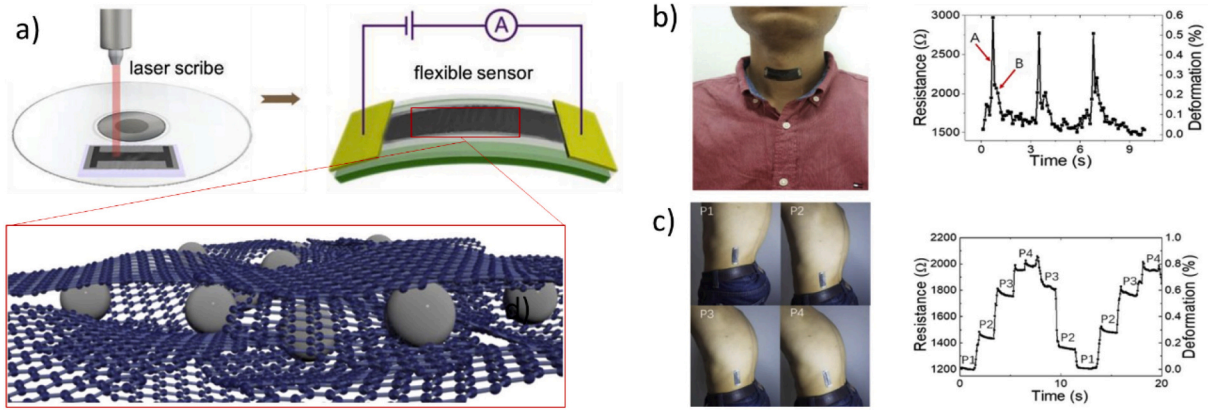

Fig. 7. a) Laser scribing process of PS nanoparticle doped rGO strain sensor. The schematic morphology of the PS nanoparticle doped rGO strain sensor is included within the red inset, b) rGO strain sensor placed on the front neck for swallowing pattern monitoring (left) and the responsive electrical signal collected by the sensor (right) and c) rGO strain sensor placed to monitor the posture of a human back (left) and the responsive electrical signal collected by the sensor (right). (Figure adapted from reference [153]).

high and reliable performance strain sensor. The tactile sensor presented a large area (8 × 8 arrays), offering a wide sensing range (1–120 kPa), sensitivity value (ΔR/R0: 0.011 kPa^{-1}), and a response time (180 ms) with excellent linearity. In addition, the device showed potential for multi-touching, tracking trajectory, and detecting shapes of external objects [157].

4.2. *Wearable sensors*

Continuous and real-time monitoring of physiological parameters and biomarkers is a powerful tool in chronic and degenerative diseases for their diagnosis, management, and treatment [158]. In that line, implantable and wearable sensors offer great promise to high quality and easy continuous monitoring; therefore, great efforts have been made in the last decades to miniaturize such biomedical sensors for human

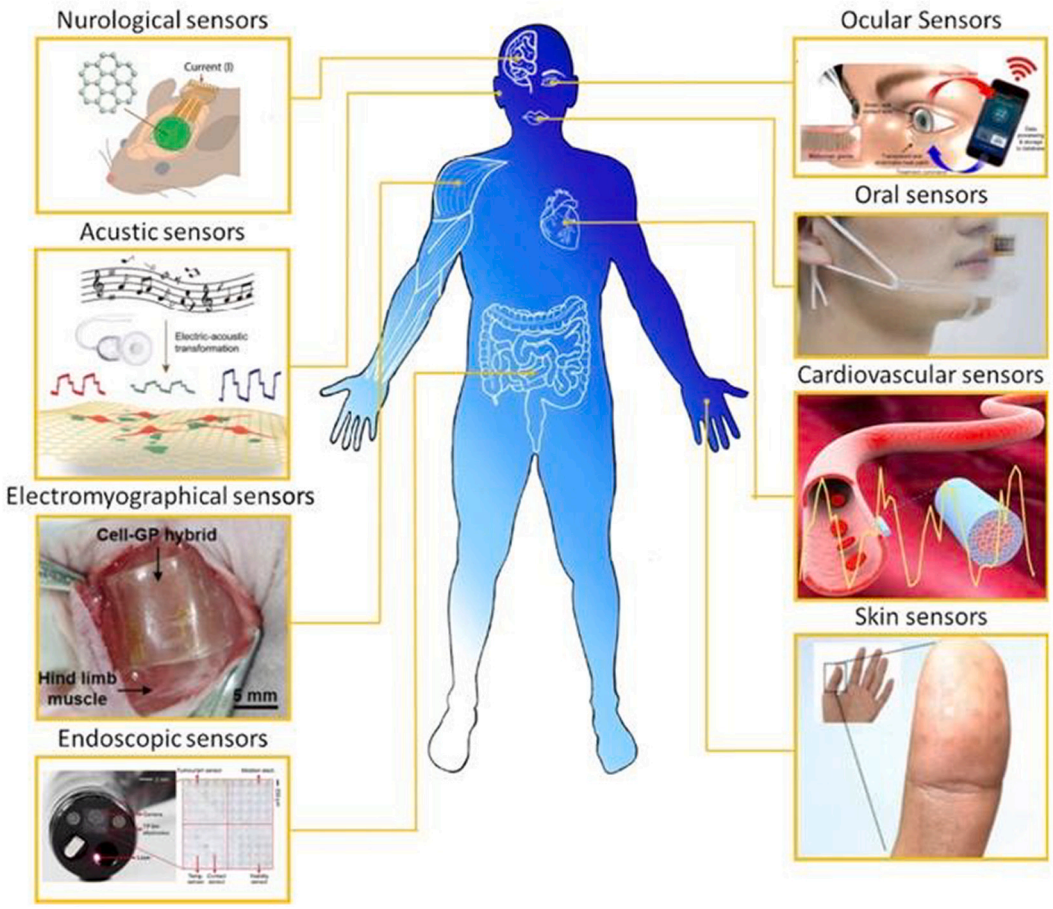

Fig. 8. Summary of wearable and implantable 2D materials-based sensor or health monitoring and of the tissues/organs monitored up to date. Reprinted with permission of ref. [164].

organ implantation [159]. Ultrathin 2D conductors and semiconductors have become ideal candidates for producing a large variety of implantable and wearable bioelectronics, given their sensitivity, fast response, long-term stability, transparency, flexibility and biocompatibility [160,161]. Among them, graphene and MoS_2 have been the most explored ones for sensing multiple organs or tissue (Fig. 8) [162–166].

The architecture of the sensing devices is crucial to simultaneously detect efficiently low and transient concentrations of analytes and avoid immune response in *in vivo* sensing. FET, electrochemical biosensors and piezoresistors are suggested as the most suitable devices, given their operation in a point-of-care manner, fast response, and low limit of detection [167]. Graphene FETs (gFET) are composed of a CVD layer of graphene deposited between two metallic electrodes, resulting in extraordinary charge mobility, high transconductance, low intrinsic noise and sensitive detection with an elevated signal-to-noise ratio [168]. Electrochemical biosensors give in real-time information about the chemical composition of a system, by coupling a specific biological or chemical receptor to an electrochemical transducer. Graphene and 2D materials have been successfully used to develop this kind of efficient transducing platform, since they offer several options to immobilize the recognition biomolecule [169,170]. Finally, piezoresistors have been used for strain and force sensors. The layered structure of 2D materials confers them with elevated GF, which are reflected in high sensitivity of the devices [62]. Sensors have been applied in multiple organs and tissues of the human body for multiple purposes. Among them, the skin is the most accessible and largest tissue and allows non-invasive monitoring; therefore, it is not surprising that most publications evaluating wearable or implantable sensors have been applied to the skin to

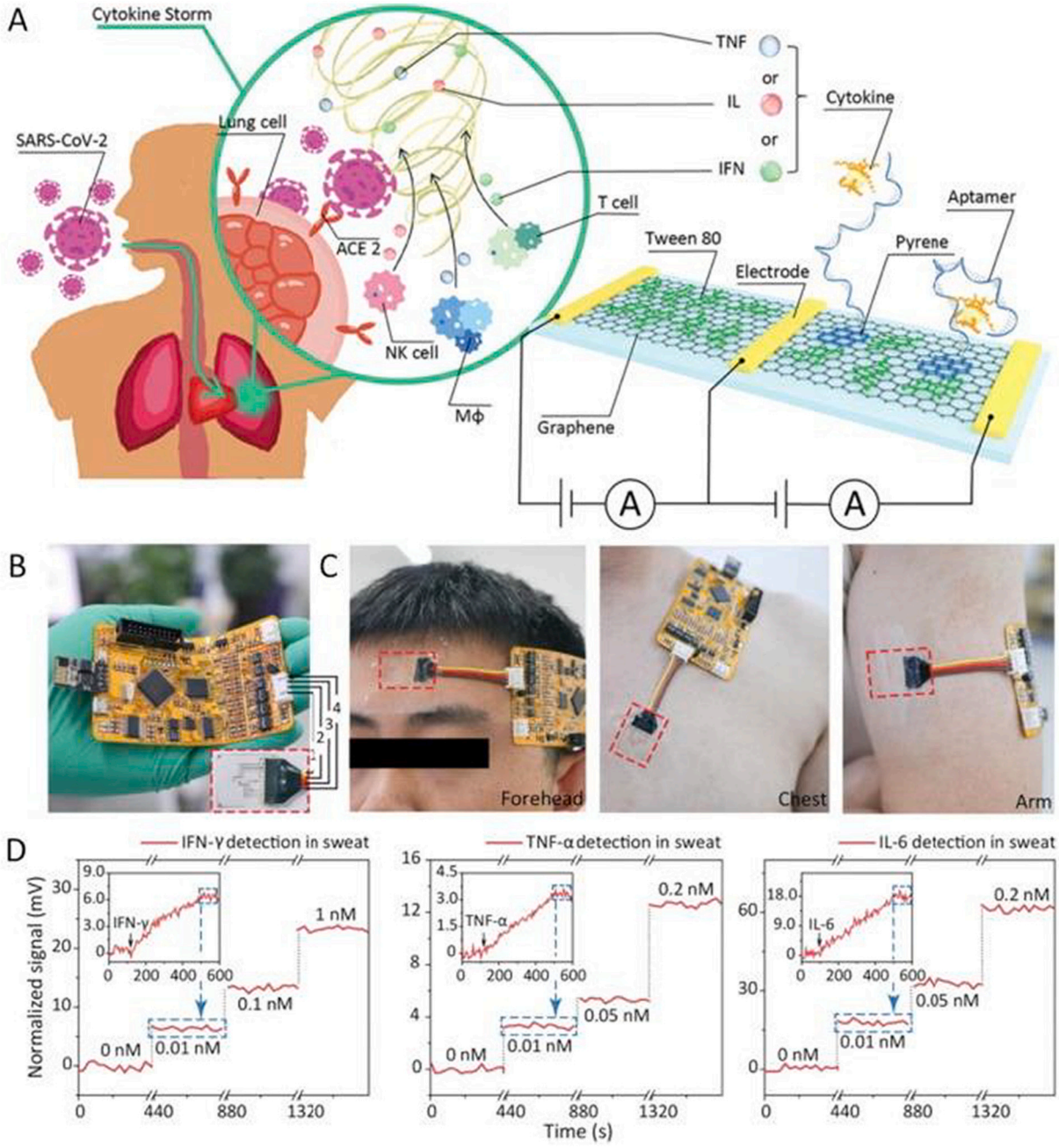

Fig. 9. (a) Scheme of the aptameric dual channel gFET biosensor for the detection of cytokine storm syndrome caused by COVID-19. (b) Photograph of the flexible and wearable aptameric gFET device. (c) The device is worn on different human body parts, e.g., forehead, chest, and arm. (h) Time-resolved and in real-time measurement of IFN, TNF, and IL-6 in human sweat. Adapted from ref. [180], Copyright 2021 Wiley.

monitor motion and vital bio-signals [171].

4.2.1. Biosensors

Biosensors can be achieved by chemically modifying 2D materials, with multiple receptors, such as antibodies, enzymes, and aptamers, to provide high specificity towards several bio-analytes [172]. In this section, we will review the most advanced technologies used for detecting a large variety of body analytes in sweat, saliva and tears and the detection of neurotransmitters.

4.2.1.1. Chemicals in sweat. Sweat is one of the most accessible biological fluids and very rich in biomolecules, such as hormones, ions, proteins and metabolites. For this reason, it is very attractive for the diagnosis of diabetes, chronic stress [173], dehydration, anaerobic metabolism, hypokalemia, hyponatremia and cystic fibrosis [174,175]. Glucose sensors are among the most studied biochemical sensors [176]. They allow non-invasive real-time monitoring of glucose levels in chronic diabetes, which are directly related to the amount of glucose in the blood. In recent studies, skin chemical sensors of graphene were developed to detect low traces of glucose, thus avoiding the current blood extraction for the same purpose [177]. Such devices are based on the electrochemical oxidation of glucose through enzymatic or non-enzymatic sensing, in which graphene is employed as an electrode. Furthermore, graphene can also be used to detect the oxidation of H_2O_2, an intermediate product of the enzymatic process of glucose. For such a purpose, Lee and co-workers fabricated a multifunctional device based on a bilayer structure of gold-doped CVD graphene modified with glucose oxidase [178]. In addition, the device was implemented with drug-loaded microneedles that where thermically activated when the sensor exceeded a glucose threshold. The authors demonstrated accurate electrical signals from the skin of two healthy volunteers and therapeutic effects on diabetic mice models. Similarly, but not in sweat, the electrochemical investigation of the MXenes with Pt nanoparticles was developed for the analysis of a wide range of molecules but in particular for the detection of H_2O_2 [179].

One relevant example of sweat sensing has been recently reported by Hao *et al.*, who developed an aptameric dual channel gFET, shown in Fig. 9, for the in-situ detection of several cytokines in COVID-19 patients, with high specificity and LOD around $600 \cdot 10^{-15}$ M [180]. Note that abnormally elevated levels of cytokines are considered prognosis biomarkers for severe or critical progression of COVID-19, and their early detection facilitates treatment to patients before they become critically ill. The device was fabricated on flexible substrates and integrated into a wireless system to enable continuous monitoring of cytokines in hospitalized patients. Apart from sweat, the gFET sensing capability toward the target cytokines was also tested in different biofluids, including plasma, saliva, and urine.

MoS_2 ultrasensitive electrochemical dopamine sensor based on manganese-doped synthesized *via* a scalable two-step approach was reported for Lei and co-workers. The authors found a selective dopamine detection with a detection limit of 50 pM in buffer solution, 5 nM in 10% serum, and 50 nM in artificial sweat [181].

4.2.1.2. Sensing in saliva. Human saliva is another interesting corporal fluid for non-invasive diagnostics and monitoring. As sweat, it is very rich in several biomarkers, *e.g.*, glucose, lactate, phosphate, hormones, proteins, and antibodies, whose abnormal concentrations can be correlated to multiple diseases, such as stress, infectious diseases, or cancer [182]. However, only a few examples in the literature of graphene-based wearable and implantable sensors for saliva exist, being most of the work focused on *ex vivo* sensing. Mannoor *et al.* developed a salivary bacterium graphene sensing platform for tooth enamel [183]. Graphene was functionalized with antimicrobial peptides to selectively bind bacteria in saliva and printed on a water-soluble silk substrate to allow the easy transfer to the tooth enamel. Furthermore, the authors integrated an inductive coil antenna in the device to allow wireless monitoring. Apart from bacteria detection, the proposed device was used for real-time monitoring of respiration.

4.2.1.3. Tears. Another rich, useful, and available fluid in the human body is the tears. Therefore, one branch of the biochemical sensors is devoted in fabricating contact lenses implemented with biochemical sensors as a non-invasive and continuous detection tool of metabolites in tears. Such ocular prostheses have specific requirements in their design, including high softness, flexibility and transparency, to perfectly adapt to the hemispherical curvature of the eye and the retina and allow a clear vision.

As in sweat sensors, glucose has been one of the main targets in this kind of smart lenses, aimed at the real-time diagnosis and monitoring of diabetic patients. For instance, Kim *et al.* developed a transparent and stretchable sensor composed of glucose oxidase-modified CVD graphene film (gFET) deposited on metal nanowires contact and integrated into soft contact lenses for wireless detection for this purpose [166]. The authors demonstrated the feasibility of their smart lenses through *in vivo* detection on a rabbit eye.

In a second application, smart lenses can also be useful in the remote monitoring and therapy of chronic ocular surface inflammation (OSI). Jang *et al.* constructed a gFET-integrated lens functionalized with antigen binding fragments (Fab) of immunoglobulin G (IgG) for the quantitative and selective detection of metalloproteinase-9 (MMP-9), a known biomarker for OSI diagnosis [165]. In addition, the authors implemented the system with an eyelid heat patch for hyperthermia treatment, connecting both diagnosis and therapeutic devices wirelessly: with the increased detection of MMP-9, the patch was heated, yielding to the lipid expression of the meibomian gland and, therefore, relieving the symptoms of OSI.

4.2.1.4. Detection of neurotransmitters. In the recent years, graphene and MoS_2-based electronics have been widely applied in the development of innovative neural interfaces [184]. Detection of brain biomolecules, and in particular neurotransmitters, has been pointed out as a promising tool to achieve a better understanding of brain functionality, as well as diagnosis and treatment of several neurodegenerative diseases. 2D materials emerged as promising candidates for building new neural interfaces that combine flexibility and transparency with suitable electronic properties and good biocompatibility.

Graphene neural implants can be classified into two subclasses: electrodes and transistors. The first example was published in 2016, in which real-time detection of dopamine in mice brain was achieved with high sensitivity and response rate using a carbon fiber microelectrode modified with electropolymerized PEDOT/rGO composite. The addition of the conductive composite not only increases the surface area but also the presence of rGO allows the adsorption of the oxidation quinone containing products, shown to be able to catalyse the dopamine-electrode electron transfer, thus resulting in a significative enhancement of the LOD [185].

Regarding multichannel devices, Liu and co-workers developed a multielectrode array as a neural probe to detect H_2O_2 produced during ischemic cascade in a rat model [186]. The device was composed of an rGO-gold oxide (rGO/Au_2O_3) nanocomposite and showed good selectivity, even in the presence of common interferences as glucose and dopamine, fast response, and low limit of detection. In addition, such architecture allowed further validation of the functional neuronal changes by recording neural evoked potentials characteristic of ischemic stroke, thus simultaneously monitoring electrophysiological and chemical signals.

On the other hand, acetylcholine (ACh) plays an important role in regulating body function, and recently, Dai *et al.* proposed a neurotransmitter molecular nanogap device composed of BP electrodes, which could distinguish the ACh from other central neurotransmitters at a low

positive bias. It has been experimentally verified in the linear sweep voltammetry (LSV) [187].

4.2.2. Wearable sensors

Physiological signals, which are generated during the body functioning, hold information about the state of the functioning of physiological systems. More specifically, electrophysiology studies the electrical properties of cells and tissues by measuring the voltage changes or electrical currents from single ion channel proteins to whole organs. The monitoring and analyses of such signals are, therefore, of great interest for the diagnosis and follow-up of a large variety of diseases.

4.2.2.1. Electrophysiological signals. The cardiovascular system generates multiple electrophysiological signals or biopotentials that can be detected non-invasively through the skin. Such activity, analysed through electrocardiograms (ECG), is currently recorded with Ag/AgCl wet electrodes, where the conductive gel is required between electrodes and the skin. However, such gels are easy to deteriorate, strongly affected by patient movements and can cause skin reactions and allergies. In order to overcome such drawbacks, multiple scientists fabricated dry-electrode devices based on 2D materials able to measure ECG [188]. Among them, it is worth mentioning the work of Akinwande *et al.*, who developed the first graphene-based electronic tattoo (GET) sensor with a thickness of 463±30 nm for ECG measurements [189]. The GET system worked as a temporary transfer tattoo; the authors proved that the recording performed on the human chest were analogous to the commercial gel electrodes. Apart from the simple preparation, the main advantage of the GET technology is the softness, which allows to obtain reproducible signals also during natural skin stretches and movements. In the same line, but not wearable sensor, a novel electrochemical aptasensor based on gold nanoparticles decorated on boron nitride nanosheets for the sensitive and selective detection of myoglobin was developed by Adeel and co-workers [190].

A second type of electrophysiological signal that is easy to monitor is the electromyography (EMG), *i.e.*, the muscle response or electrical activity in response to a nerve's stimulation of the muscle. One of the few examples in the literature is based on a wireless nanomembrane device based on ultrathin, low-profile, lightweight, soft, and stretchable graphene sensors that could be laminated to the skin over the target muscle to record EMG activity on free moving mice during mastication [191].

The current trend is to move towards multidevice arrays architectures to enhance the spatial and temporal resolution of the devices. With them, simultaneous recording and stimulation of brain activity can be done. For instance, a 16-channel electrodes flexible array composed of 4-layers graphene was used to stimulate the mice brain and simultaneously record calcium imaging [192]. Such a tool exhibited great potential for the treatment of neurodegenerative diseases (Fig. 10).

4.2.2.2. Human motion. Body motions can be monitored through pressure and mechanical stress using strain or piezoelectric pressure sensors. In fact, 2D materials, and in particular MXenes, gained increased attention in this application as they can offer a piezoelectric effect with high GF, thus showing high sensitivity [62,193,194]. The main challenge is to ensure proper adhesion to the skin in both dry and wet conditions. In fact, most of the sensors employed for monitoring body movements are also used to record ECG signals and other mechanical motions, such as speech vibrations or respiration [195].

One of the most interesting examples was a tactile fingerprint sensor produced by Park and co-workers [156]. The authors used MoS_2 over CVD grown graphene electrodes to fabricate a very flexible, transparent, and ultrathin sensor of 75 nm that was perfectly adaptable to the tiny imperfections of the skin, including fingerprints. Such technology has great potential to restore human functions, such as tactile sensibility lost in damaged or burned skin. In a second example, a wearable piezoresistor made of palladium nano-islands on single-layer graphene was employed to monitor swallowing ability in patients after cancer radiation therapy, who might present reduced swallowing activity and dysphagia [196]. Furthermore, the authors implemented their technology with machine-learning to distinguish among other body motion signals, coming from coughing, turning of the head, and swallowing boluses of different consistencies.

4.2.2.3. Breath monitoring. The analysis of the amount and quality of respiration is the most critical and real-time monitored signal to understand if hospitalized patients are taking proper, healthy breaths. Commonly, a wearable mask implemented with a strain sensor is used to detect the pressure changes in the breathing airflow. Graphene-related materials have been shown to provide a large working range and elevated sensitivity, a key requirement for this application. Among the large diversity of substrates, graphene-based textile and paper sensors are lately employed for respiration monitoring, as they are low-cost, easy to prepare, soft and green materials [197,198]. In one example, tissue paper was soaked into GO and then reduced through a thermal approach [199]. The resulting device exhibited high sensitivity (17.2 kPa^{-1}) and a large working range (0−20 kPa), allowing also pulse

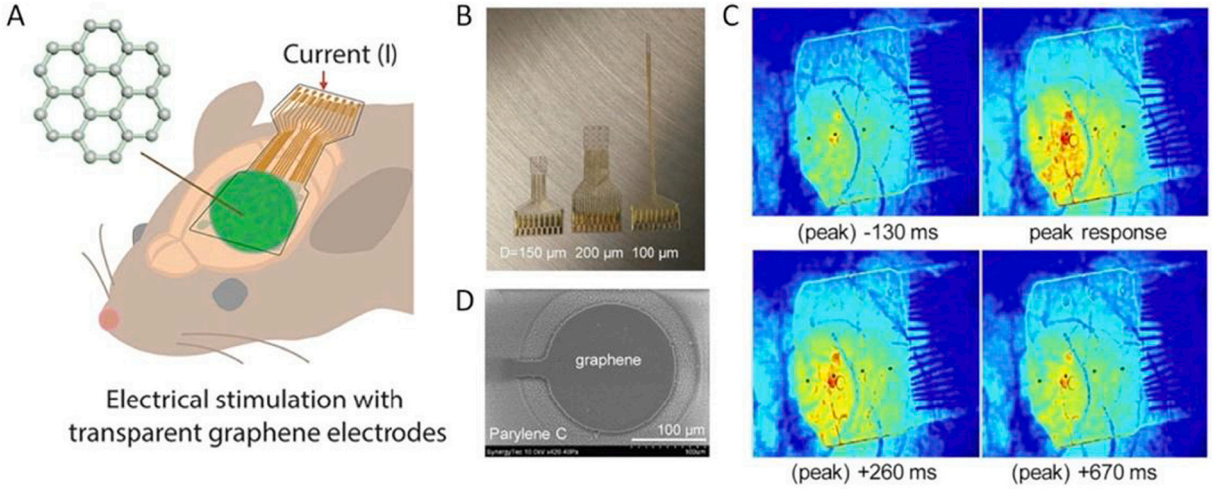

Fig. 10. (a) Representation of multielectrode array implantation over motor cortex for electrical stimulation in mice model; (b) Three different kinds of neural probes. (c) SEM image of graphene electrode. (d) Calcium imaging fluorescence visualization of the intensity of neural response at different time points. Reproduced from ref. [192], Copyright 2018 American Chemical Society.

detection, voice recognition, and intense motion detection.

In another approach, strain sensors can be attached to the chest of the patient and, usually, can havedual functionality. For instance, Ramirez and co-workers developed a graphene/palladium device supported on PEDOT:PSS to monitor simultaneously respiration and heartbeat [200]. The resulting sensor exhibited high sensitivity at low strains and an extensive working range (up to 86%), which are essential to detect heartbeat (small strain, shorter time interval) and respiration (large strain, longer time interval) at the same time (Fig. 11).

An alternative to strain sensors in breath monitoring are humidity sensors, which measure the relative humidity differences between exhalation and inhalation. Among the diverse 2D materials, GO is the most widespread, given the large surface area and superpermeability of water molecules. Moreover, GO can promote protons generation in contact with water. For instance, He and co-workers developed a wireless humidity sensor composed of polydopamine and GO that was based on the continuous binding and unbinding of H-bonds between the polymer and water molecules [201]. This kind of sensing devices exhibit a very low impedance, high sensitivity, ultrafast response, and reduced hysteresis, thus allowing real-time respiratory detection of slow, medium, and rapid breathing. On the other side, WS_2 films have also shown great humidity sensing performance, with a rapid response and sensitivity good enough to allow mask-free monitoring [202].

4.2.2.4. Sound and voice sensing. In the past years, the interest in speech recognition for human-machine interaction and speech ability recovering has increased significantly. Multiple works have been published where pressure sensors with multiple architectures and supports have been upgraded with ultra-high sensitivity, required to capture the subtle muscle movement during speech and rapid response speed [164]. However, probably the most innovative and avant-garde work, published a couple of years ago, is a wearable artificial throat built with LIG on polyimide substrate able to simultaneously detect and generate sounds (Fig. 12) [203]. The technology showed outstanding properties (high sensitivity, low limit detection, high thermal conductivity, and low heat capacity) for the thermoacoustic sound sources. The authors, in addition, demonstrated its ability to recognize different intensities and volumes of hum, cough, and scream, convert those unclear throat vibrations into controllable sounds and, thus, differentiate between different pronounced words and sentences. Overall, this work is considered the starting point towards specific phonation recognition, aiding and speech rehabilitation training for disabled patients.

4.2.2.5. Photosensing. Apart from piezo-resistivity, which is useful to produce highly sensitive strains and force sensors, some 2D materials, such as metal dichalcogenides, have a unique photo-absorption and photocurrent properties, which can be interesting for optoelectronic devices [30,204]. In particular, MoS_2 has been used to fabricate efficient phototransistors with elevated sensitivity and ultrafast response times (below 50 ms) [205,206]. In one application, such devices can be applied as artificial retinas: the synapses happening in the retina have a light evoked excitatory and inhibitory behavior; MoS_2 and 2D perovskite are able to transduce light pulses into electrical signals, thus functioning as artificial synapses. Chansoon and co-workers developed a hemispherical curved soft optoelectronic device inspired by the human eye using ultrathin CVD MoS_2 and graphene films [207]. Under illumination, the image sensor generates a photocurrent that is proportional to the incident light intensity, while allowing aberration free imaging and a wide field of view (Fig. 13). Furthermore, the captured image was not affected by the IR radiation from the blindness of the MoS_2-based phototransistor, originating from material bind gaps. The authors demonstrated its feasibility when implanted in rat eyes, showing that attached to the retina, this device successfully stimulated the optic nerves and then transferred to the visual cortex.

5. Conclusions and future perspectives

In this review, we have discussed numerous examples in which 2D materials contribute to developing physical, chemical, bio and wearable sensors. The large contact surface area in a small volume ratio is one of the key points for this type of 2D-based sensors, achieving a good limit of detection (LOD) and sensitivity.

In the chemical and physical sensors applications, the selection of the 2D material sensing platform plays an important role. The use of pristine and defect-free materials may alter the selectivity of the device. For this reason, the presence of anchor groups onto the surface can favor the analyte absorption. In chemiresistive devices, the application more extended is gas sensing, and authors have focused mainly on NO_2, NH_3 and humidity sensors. The field requires looking forward to other toxic gases in industry, but other approaches aside from *n*- or *p*-doping are needed. The role of decorating 2D materials with metals in optical-based devices has also been reviewed. Their combination helps to facilitate electron transfer processes, improve the selectivity and sensitivity and enhance the limit of detection of sensors. For piezoresistive devices, graphene has demonstrated great potential for artificial electronic skins, human activity detection, health monitoring and wearable applications. However, micro-manufacturing and processing in sub-microscale on flexible substrate is still a challenge and represent its main drawback. In the case of 2D TMD-based materials for flexible electronics, the field requires advancements, including new synthetic pathways, new techniques in device fabrication and improvement in the material-substrate interaction. Tungsten and molybdenum 2D materials are the most

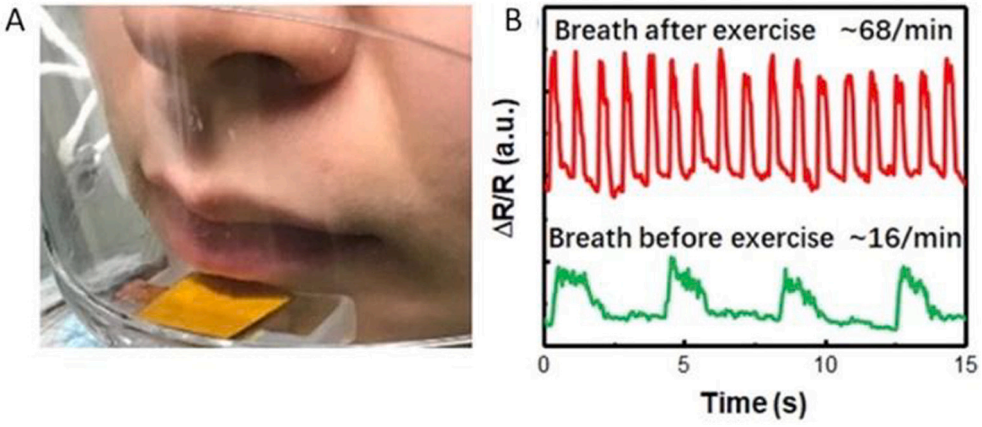

Fig. 11. (a) Application for respiration detection. (b) Response curves for breathing before and after exercise. Reproduced from ref. [199], Copyright 2017 American Chemical Society.

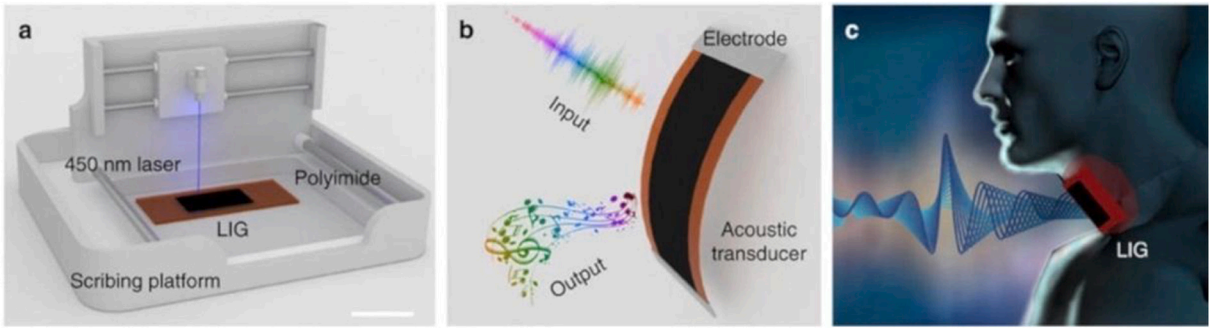

Fig. 12. Schematic representation of the graphene-based artificial throat (a) One-step LIG fabrication. PI is converted into LIG by laser irradiation at 450 nm (Scale bar, 2.5 cm). (b) LIG has both the ability of emitting and detecting sounds. (c) The artificial throat is able to detect the movement of the throat, generating controllable sounds [203].

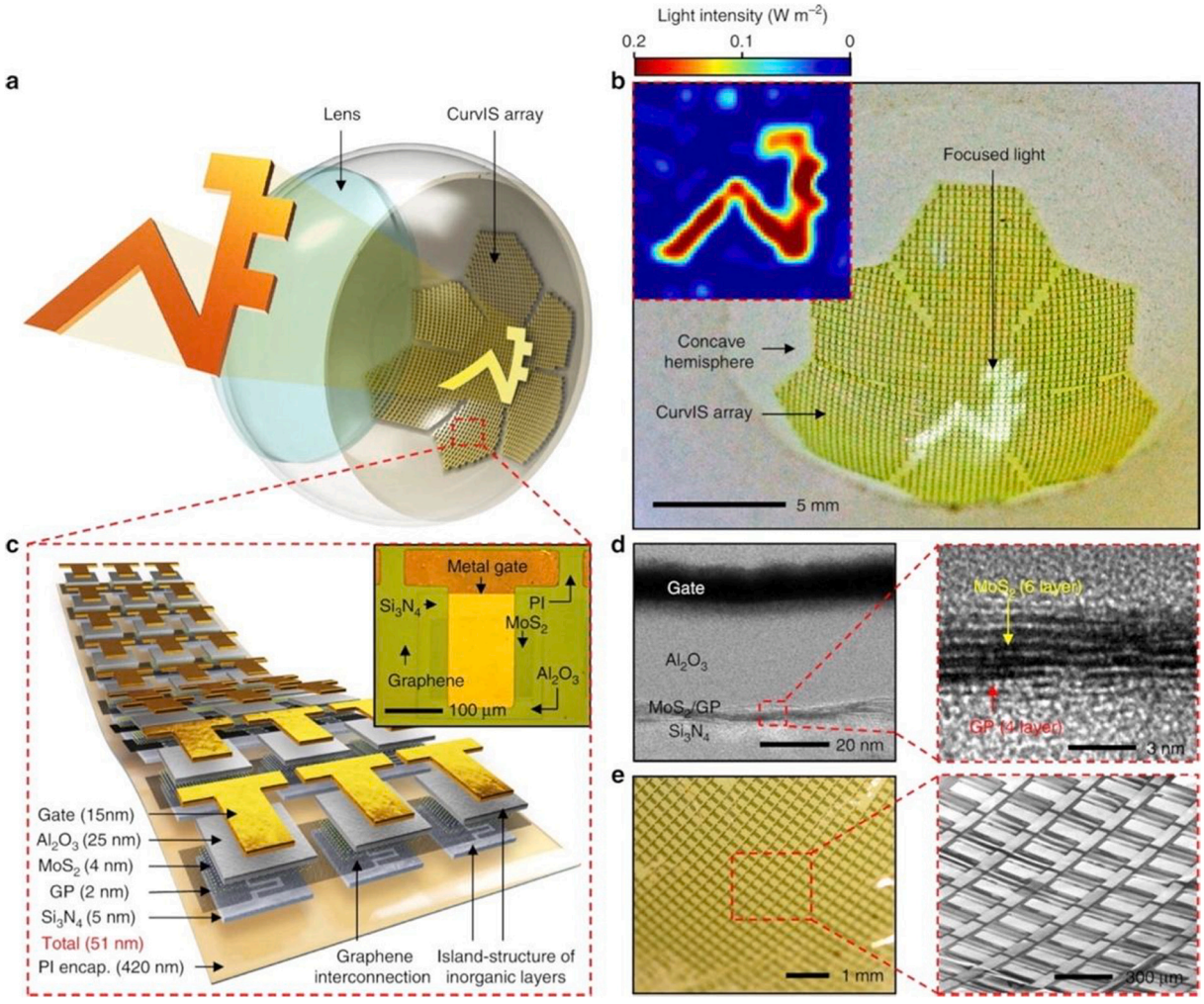

Fig. 13. CurvIS array based on MoS_2-graphene heterostructure. (a) Schematic illustration of the CurvIS. (b) Optical image of the device. In the inset is shown the image captured by the CurvIS array. (c) Schematic illustration of the layered structure of the device. In the inset is represented an optical microscope image of a single phototransistor. (d) Transmission electron microscope image of the MoS_2-graphene phototransistor cross-section. (e) Optical (left) and magnified scanning electron microscope (right) image of the high-density CurvIS array mounted on the concave hemisphere. Reproduced from ref. [207], Copyright 2017 Nature.

explored, while tellurides and other 2D members, such as h-BN and BF remain much less explored.

Besides, the research of graphene-based sensors for skin has made remarkable achievements, but there still exist some limitations that nanomaterials are not solving yet. Except for a few examples, most 2D sensing derivatives cannot detect target analytes by themselves, so they are often modified with biomolecules. This fact limits their applications because it increases production costs, in addition to their poor stability.

Even though the biocompatibility of some implantable 2D materials-based biomedical devices *in vitro* has been demonstrated, the main challenge for their clinical use is their *in vivo* biocompatibility. Biomimetic mechanical properties or coating with biocompatible materials

have been shown to reduce inflammation and immune responses. The long-term stability and functionality of both wearable and implantable devices are essential for possible commercialization. Regarding cytotoxicity, only a few studies have been published about the cutaneous toxicity of graphene-based or TMDs-based sensors. In general, the most likely scenario is skin irritation and allergic response, but the cause remains unclear. The current challenge for 2D materials concerning biosensing is the improvement of reproducibility between devices.

Every year new sensing platforms are described, and the field is advancing quickly. The next horizons are multiplatform sensing through the combination of various materials. The formation of cross-linked heterostructures not only for 2D-2D blocks but also with other low-dimensional materials is becoming an important topic, producing unprecedented features that cannot be reached by individual 2D counterparts [220,221].

Research on 2D materials has been going on for 18 years since it was first proposed, and all the works in literature pave the way and leave no doubt about the potential of 2D materials for applications in sensing. But, up to now, we cannot find so many products containing 2D materials in the market. Albeit it is challenging, the researcher's long-term goal is moving towards the commercialization of sensing devices containing 2D materials [222]. In this regard, achieving a reliable product design, scalability and low-cost production are the key industrial aspects of being in the market. 2D materials, such as graphene, TMDs, and their heterostructures, are considered the most viable candidates for industrial fabrication. An Industry-University Cooperative Research Centre has achieved scalable synthesis and sensor fabrication methods for the electrodeposition of TMDs (Atomically Thin Multifunctional Coatings).

Nonetheless, nowadays, the deposition and growth of 2D materials can be suitable for wafer-scale. Still, defects and contamination are not yet in line with manufacturing standards and only partially meet industrial specifications. Addressing these critical manufacturing obstacles is the clear goal of the European 2D materials pilot line.

Declaration of Competing Interest

The authors declare that they have no known competing financial interests or personal relationships that could have appeared to influence the work reported in this paper.

Data availability

No data was used for the research described in the article.

Acknowledges

I. J. Gómez acknowledges the Operational Program Research, Development, and Education-Project 'MSCAfellow4@MUNI' (No. CZ.02.2.69/0.0/0.0/20_079/0017045). Antonio Dominguez-Alfaro thanks Margarita Salas Postdoctoral Fellowship at the University of the Basque Country (UPV/EHU), financed by the European Union – Next Generation EU Funds. A. Silvestri thanks Grants FJC2018-036777-I funded by MCIN/AEI/10.13039/501100011033. Part of this work was performed under the Maria de Maeztu Units of Excellence Program from the Spanish State Research Agency – grant no. MDM-2017-0720.

References

[1] F. Arduini, S. Cinti, V. Scognamiglio, D. Moscone, G. Palleschi, How cutting-edge technologies impact the design of electrochemical (bio)sensors for environmental analysis. A review, Analyt. Chim. Acta 959 (2017) 15–42, https://doi.org/10.1016/j.aca.2016.12.035.

[2] X. Chen, M. Leishman, D. Bagnall, N. Nasiri, Nanostructured gas sensors: from air quality and environmental monitoring to healthcare and medical applications, Nanomaterials (2021), https://doi.org/10.3390/nano11081927.

[3] D. Tyagi, H. Wang, W. Huang, L. Hu, Y. Tang, Z. Guo, Z. Ouyang, H. Zhang, Recent advances in two-dimensional-material-based sensing technology toward health and environmental monitoring applications, Nanoscale 12 (6) (2020) 3535–3559, https://doi.org/10.1039/C9NR10178K.

[4] P. Miró, M. Audiffred, T. Heine, An atlas of two-dimensional materials, Chem. Soc. Rev. 43 (18) (2014) 6537–6554, https://doi.org/10.1039/C4CS00102H.

[5] S. Radhakrishnan, M. Mathew, C.S. Rout, Microfluidic sensors based on two-dimensional materials for chemical and biological assessments, Mat. Adv. 3 (4) (2022) 1874–1904, https://doi.org/10.1039/D1MA00929J.

[6] Q.-N. Zhao, Y.-J. Zhang, Z.-H. Duan, S. Wang, C. Liu, Y.-D. Jiang, H.-L. Tai, A review on $Ti_3C_2T_x$-based nanomaterials: synthesis and applications in gas and humidity sensors, Rare Metals 40 (6) (2021) 1459–1476, https://doi.org/10.1007/s12598-020-01602-2.

[7] A. García-Miranda Ferrari, S.J. Rowley-Neale, C.E. Banks, Recent advances in 2D hexagonal boron nitride (2D-hBN) applied as the basis of electrochemical sensing platforms, Anal. Bioanal. Chem. 413 (3) (2021) 663–672, https://doi.org/10.1007/s00216-020-03068-8.

[8] K.S. Novoselov, A.K. Geim, S.V. Morozov, D. Jiang, Y. Zhang, S.V. Dubonos, I. V. Grigorieva, A.A. Firsov, Electric field effect in atomically thin carbon films, Science 306 (5696) (2004) 666–669, https://doi.org/10.1126/science.1102896.

[9] C.N.R. Rao, A.K. Sood, K.S. Subrahmanyam, A. Govindaraj, Graphene: the new two-dimensional nanomaterial, Angew. Chem. Int. Ed. 48 (42) (2009) 7752–7777, https://doi.org/10.1002/anie.200901678.

[10] S.S. Varghese, S.H. Varghese, S. Swaminathan, K.K. Singh, V. Mittal, Two-dimensional materials for sensing: graphene and beyond, Electronics (2015) 651–687, https://doi.org/10.3390/electronics4030651.

[11] D.J. Late, Y.-K. Huang, B. Liu, J. Acharya, S.N. Shirodkar, J. Luo, A. Yan, D. Charles, U.V. Waghmare, V.P. Dravid, C.N.R. Rao, Sensing behavior of atomically thin-layered MoS_2 transistors, ACS Nano 7 (6) (2013) 4879–4891, https://doi.org/10.1021/nn400026u.

[12] C. Tan, X. Cao, X.-J. Wu, Q. He, J. Yang, X. Zhang, J. Chen, W. Zhao, S. Han, G.-H. Nam, M. Sindoro, H. Zhang, Recent advances in ultrathin two-dimensional nanomaterials, Chem. Rev. 117 (9) (2017) 6225–6331, https://doi.org/10.1021/acs.chemrev.6b00558.

[13] X. Liu, T. Ma, N. Pinna, J. Zhang, Two-dimensional nanostructured materials for gas sensing, Adv. Funct. Mater. 27 (37) (2017) 1702168, https://doi.org/10.1002/adfm.201702168.

[14] I.J. Gómez, N. Alegret, A. Dominguez-Alfaro, M. Vázquez Sulleiro, Recent advances on 2D materials towards 3D printing, Chemistry (2021) 1314–1343, https://doi.org/10.3390/chemistry3040095.

[15] M. Zeng, Y. Xiao, J. Liu, K. Yang, L. Fu, Exploring two-dimensional materials toward the next-generation circuits: from monomer design to assembly control, Chem. Rev. 118 (13) (2018) 6236–6296, https://doi.org/10.1021/acs.chemrev.7b00633.

[16] E. Singh, M. Meyyappan, H.S. Nalwa, Flexible graphene-based wearable gas and chemical sensors, ACS Appl. Mater. Interfaces 9 (40) (2017) 34544–34586, https://doi.org/10.1021/acsami.7b07063.

[17] G.-H. Lee, R.C. Cooper, S.J. An, S. Lee, A. van der Zande, N. Petrone, A. G. Hammerberg, C. Lee, B. Crawford, W. Oliver, J.W. Kysar, J. Hone, High-strength chemical-vapor–deposited graphene and grain boundaries, Science 340 (6136) (2013) 1073–1076, https://doi.org/10.1126/science.1235126.

[18] S. Park, R.S. Ruoff, Chemical methods for the production of graphenes, Nat. Nanotechnol. 4 (4) (2009) 217–224, https://doi.org/10.1038/nnano.2009.58.

[19] Y. Hernandez, V. Nicolosi, M. Lotya, F.M. Blighe, Z. Sun, S. De, I.T. McGovern, B. Holland, M. Byrne, Y.K. Gun'Ko, J.J. Boland, P. Niraj, G. Duesberg, S. Krishnamurthy, R. Goodhue, J. Hutchison, V. Scardaci, A.C. Ferrari, J. N. Coleman, High-yield production of graphene by liquid-phase exfoliation of graphite, Nat. Nanotechnol. 3 (9) (2008) 563–568, https://doi.org/10.1038/nnano.2008.215.

[20] I.J. Gómez, M. Vázquez Sulleiro, D. Mantione, N. Alegret, Carbon nanomaterials embedded in conductive polymers: a state of the art, Polymers (2021), https://doi.org/10.3390/polym13050745.

[21] M.V. Sulleiro, S. Quiroga, D. Peña, D. Pérez, E. Guitián, A. Criado, M. Prato, Microwave-induced covalent functionalization of few-layer graphene with arynes under solvent-free conditions, Chem. Commun. 54 (17) (2018) 2086–2089, https://doi.org/10.1039/C7CC08676H.

[22] V. Nicolosi, M. Chhowalla, M.G. Kanatzidis, M.S. Strano, J.N. Coleman, Liquid exfoliation of layered materials, Science 340 (6139) (2013) 1226419, https://doi.org/10.1126/science.1226419.

[23] J.R. Prekodravac, D.P. Kepić, J.C. Colmenares, D.A. Giannakoudakis, S. P. Jovanović, A comprehensive review on selected graphene synthesis methods: from electrochemical exfoliation through rapid thermal annealing towards biomass pyrolysis, J. Mater. Chem. C 9 (21) (2021) 6722–6748, https://doi.org/10.1039/D1TC01316E.

[24] R. Mas-Ballesté, C. Gómez-Navarro, J. Gómez-Herrero, F. Zamora, 2D materials: to graphene and beyond, Nanoscale 3 (1) (2011) 20–30, https://doi.org/10.1039/C0NR00323A.

[25] S. Manzeli, D. Ovchinnikov, D. Pasquier, O.V. Yazyev, A. Kis, 2D transition metal dichalcogenides, Nat. Rev. Mat. 2 (8) (2017) 17033, https://doi.org/10.1038/natrevmats.2017.33.

[26] A. Splendiani, L. Sun, Y. Zhang, T. Li, J. Kim, C.-Y. Chim, G. Galli, F. Wang, Emerging photoluminescence in monolayer MoS_2, Nano Lett. 10 (4) (2010) 1271–1275, https://doi.org/10.1021/nl903868w.

[27] E. Wu, Y. Xie, B. Yuan, D. Hao, C. An, H. Zhang, S. Wu, X. Hu, J. Liu, D. Zhang, Specific and highly sensitive detection of ketone compounds based on p-Type $MoTe_2$ under ultraviolet illumination, ACS Appl. Mater. Interfaces 10 (41) (2018) 35664–35669, https://doi.org/10.1021/acsami.8b14142.

[28] T. Chowdhury, E.C. Sadler, T.J. Kempa, Progress and prospects in transition-metal dichalcogenide research beyond 2D, Chem. Rev. 120 (22) (2020) 12563–12591, https://doi.org/10.1021/acs.chemrev.0c00505.

[29] X. Xu, W. Yao, D. Xiao, T.F. Heinz, Spin and pseudospins in layered transition metal dichalcogenides, Nat. Phys. 10 (5) (2014) 343–350, https://doi.org/10.1038/nphys2942.

[30] K.F. Mak, J. Shan, Photonics and optoelectronics of 2D semiconductor transition metal dichalcogenides, Nat. Photonics 10 (4) (2016) 216–226, https://doi.org/10.1038/nphoton.2015.282.

[31] E. Martínez-Periñán, T. García-Mendiola, E. Enebral-Romero, R. del Caño, M. Vera-Hidalgo, M. Vázquez Sulleiro, C. Navío, F. Pariente, E.M. Pérez, E. Lorenzo, A MoS_2 platform and thionine-carbon nanodots for sensitive and selective detection of pathogens, Biosens. Bioelectron. 189 (2021), 113375, https://doi.org/10.1016/j.bios.2021.113375.

[32] A.M. Villa-Manso, M. Revenga-Parra, M. Vera-Hidalgo, M. Vázquez Sulleiro, E. M. Pérez, E. Lorenzo, F. Pariente, 2D MoS_2 nanosheets and hematein complexes deposited on screen-printed graphene electrodes as an efficient electrocatalytic sensor for detecting hydrazine, Sensors Actuators B Chem. 345 (2021) 130385, https://doi.org/10.1016/j.snb.2021.130385.

[33] K. Kang, S. Chen, E.-H. Yang, 12 - Synthesis of transition metal dichalcogenides, in: E.-H. Yang, D. Datta, J. Ding, G. Hader (Eds.), Synthesis, Modeling, and Characterization of 2D Materials, and Their Heterostructures, Elsevier, 2020, pp. 247–264, https://doi.org/10.1016/B978-0-12-818475-2.00012-X.

[34] E. Er, H.-L. Hou, A. Criado, J. Langer, M. Möller, N. Erk, L.M. Liz-Marzán, M. Prato, High-yield preparation of exfoliated 1T-MoS_2 with SERS activity, Chem. Mater. 31 (15) (2019) 5725–5734, https://doi.org/10.1021/acs.chemmater.9b01698.

[35] L. Li, Y. Yu, G.J. Ye, Q. Ge, X. Ou, H. Wu, D. Feng, X.H. Chen, Y. Zhang, Black phosphorus field-effect transistors, Nat. Nanotechnol. 9 (5) (2014) 372–377, https://doi.org/10.1038/nnano.2014.35.

[36] Y. Xu, Z. Shi, X. Shi, K. Zhang, H. Zhang, Recent progress in black phosphorus and black-phosphorus-analogue materials: properties, synthesis and applications, Nanoscale 11 (31) (2019) 14491–14527, https://doi.org/10.1039/C9NR04348A.

[37] A. Castellanos-Gomez, L. Vicarelli, E. Prada, J.O. Island, K.L. Narasimha-Acharya, S.I. Blanter, D.J. Groenendijk, M. Buscema, G.A. Steele, J.V. Alvarez, H. W. Zandbergen, J.J. Palacios, H.S.J. van der Zant, Isolation and characterization of few-layer black phosphorus, 2D, Materials 1 (2) (2014), 025001, https://doi.org/10.1088/2053-1583/1/2/025001.

[38] Y. Sui, J. Zhou, X. Wang, L. Wu, S. Zhong, Y. Li, Recent advances in black-phosphorus-based materials for electrochemical energy storage, Mater. Today 42 (2021) 117–136, https://doi.org/10.1016/j.mattod.2020.09.005.

[39] G.-Q. Zhao, J. Hu, X. Long, J. Zou, J.-G. Yu, F.-P. Jiao, A critical review on black phosphorus-based photocatalytic CO_2 reduction application, Small 17 (49) (2021) 2102155, https://doi.org/10.1002/smll.202102155.

[40] Q. Li, J.-T. Wu, Y. Liu, X.-M. Qi, H.-G. Jin, C. Yang, J. Liu, G.-L. Li, Q.-G. He, Recent advances in black phosphorus-based electrochemical sensors: a review, Anal. Chim. Acta 1170 (2021), 338480, https://doi.org/10.1016/j.aca.2021.338480.

[41] Y. Miao, X. Wang, J. Sun, Z. Yan, Recent advances in the biomedical applications of black phosphorus quantum dots, Nanoscale Adv. 3 (6) (2021) 1532–1550, https://doi.org/10.1039/D0NA01003K.

[42] S. Cui, H. Pu, S.A. Wells, Z. Wen, S. Mao, J. Chang, M.C. Hersam, J. Chen, Ultrahigh sensitivity and layer-dependent sensing performance of phosphorene-based gas sensors, Nat. Commun. 6 (1) (2015) 8632, https://doi.org/10.1038/ncomms9632.

[43] A.N. Abbas, B. Liu, L. Chen, Y. Ma, S. Cong, N. Aroonyadet, M. Köpf, T. Nilges, C. Zhou, Black phosphorus gas sensors, ACS Nano 9 (5) (2015) 5618–5624, https://doi.org/10.1021/acsnano.5b01961.

[44] S.-Y. Cho, Y. Lee, H.-J. Koh, H. Jung, J.-S. Kim, H.-W. Yoo, J. Kim, H.-T. Jung, Superior chemical sensing performance of black phosphorus: comparison with MoS_2 and graphene, Adv. Mater. 28 (32) (2016) 7020–7028, https://doi.org/10.1002/adma.201601167.

[45] E. Akbarnejad, F. Salehi, S. Mohajerzadeh, Facile and rapid exfoliation of black phosphorus assisted by acetic acid, J. Mater. Sci. Mater. Electron. 33 (5) (2022) 2499–2508, https://doi.org/10.1007/s10854-021-07457-2.

[46] Y. Zeng, Z. Guo, Synthesis and stabilization of black phosphorus and phosphorene: Recent progress and perspectives, iScience 24 (10) (2021), https://doi.org/10.1016/j.isci.2021.103116.

[47] L. Song, L. Ci, H. Lu, P.B. Sorokin, C. Jin, J. Ni, A.G. Kvashnin, D.G. Kvashnin, J. Lou, B.I. Yakobson, P.M. Ajayan, Large scale growth and characterization of atomic hexagonal boron nitride layers, Nano Lett. 10 (8) (2010) 3209–3215, https://doi.org/10.1021/nl1022139.

[48] J.D. Caldwell, I. Aharonovich, G. Cassabois, J.H. Edgar, B. Gil, D.N. Basov, Photonics with hexagonal boron nitride, Nat. Rev. Mat. 4 (8) (2019) 552–567, https://doi.org/10.1038/s41578-019-0124-1.

[49] X. Chen, S. Lin, H. Zhang, Screening of single-atom catalysts sandwiched by boron nitride sheet and graphene for oxygen reduction and oxygen evolution, Renew. Energy 189 (2022) 502–509, https://doi.org/10.1016/j.renene.2022.03.003.

[50] S. Roy, X. Zhang, A.B. Puthirath, A. Meiyazhagan, S. Bhattacharyya, M. M. Rahman, G. Babu, S. Susarla, S.K. Saju, M.K. Tran, L.M. Sassi, M.A.S.R. Saadi, J. Lai, O. Sahin, S.M. Sajadi, B. Dharmarajan, D. Salpekar, N. Chakingal, A. Baburaj, X. Shuai, A. Adumbumkulath, K.A. Miller, J.M. Gayle, A. Ajnsztajn, T. Prasankumar, V.V.J. Harikrishnan, V. Ojha, H. Kannan, A.Z. Khater, Z. Zhu, S. A. Iyengar, P.A.D.S. Autreto, E.F. Oliveira, G. Gao, A.G. Birdwell, M.R. Neupane, T.G. Ivanov, J. Taha-Tijerina, R.M. Yadav, S. Arepalli, R. Vajtai, P.M. Ajayan, Structure, properties and applications of two-dimensional hexagonal boron nitride, Adv. Mater. 33 (44) (2021) 2101589, https://doi.org/10.1002/adma.202101589.

[51] Y. He, D. Li, W. Gao, H. Yin, F. Chen, Y. Sun, High-performance NO_2 sensors based on spontaneously functionalized hexagonal boron nitride nanosheets via chemical exfoliation, Nanoscale 11 (45) (2019) 21909–21916, https://doi.org/10.1039/C9NR07153A.

[52] X. Li, X. Hao, M. Zhao, Y. Wu, J. Yang, Y. Tian, G. Qian, Exfoliation of hexagonal boron nitride by molten hydroxides, Adv. Mater. 25 (15) (2013) 2200–2204, https://doi.org/10.1002/adma.201204031.

[53] C. Gautam, S. Chelliah, Methods of hexagonal boron nitride exfoliation and its functionalization: covalent and non-covalent approaches, RSC Adv. 11 (50) (2021) 31284–31327, https://doi.org/10.1039/D1RA05727H.

[54] M. Naguib, M. Kurtoglu, V. Presser, J. Lu, J. Niu, M. Heon, L. Hultman, Y. Gogotsi, M.W. Barsoum, Two-dimensional nanocrystals produced by exfoliation of $Ti3AlC_2$, Adv. Mater. 23 (37) (2011) 4248–4253, https://doi.org/10.1002/adma.201102306.

[55] O. Mashtalir, M. Naguib, V.N. Mochalin, Y. Dall'Agnese, M. Heon, M.W. Barsoum, Y. Gogotsi, Intercalation and delamination of layered carbides and carbonitrides, Nat. Commun. 4 (1) (2013) 1716, https://doi.org/10.1038/ncomms2664.

[56] L. Verger, C. Xu, V. Natu, H.-M. Cheng, W. Ren, M.W. Barsoum, Overview of the synthesis of MXenes and other ultrathin 2D transition metal carbides and nitrides, Curr. Opinion Solid State Mater. Sci. 23 (3) (2019) 149–163, https://doi.org/10.1016/j.cossms.2019.02.001.

[57] M. Naguib, O. Mashtalir, J. Carle, V. Presser, J. Lu, L. Hultman, Y. Gogotsi, M. W. Barsoum, Two-dimensional transition metal carbides, ACS Nano 6 (2) (2012) 1322–1331, https://doi.org/10.1021/nn204153h.

[58] Z. Meng, R.M. Stolz, L. Mendecki, K.A. Mirica, Electrically-transduced chemical sensors based on two-dimensional nanomaterials, Chem. Rev. 119 (1) (2019) 478–598, https://doi.org/10.1021/acs.chemrev.8b00311.

[59] Y. Wang, Y. Shao, D.W. Matson, J. Li, Y. Lin, Nitrogen-doped graphene and its application in electrochemical biosensing, ACS Nano 4 (4) (2010) 1790–1798, https://doi.org/10.1021/nn100315s.

[60] A. Silvestri, A. Criado, F. Poletti, F. Wang, P. Fanjul-Bolado, M.B. González-García, C. García-Astrain, L.M. Liz-Marzán, X. Feng, C. Zanardi, M. Prato, Bioresponsive, electroactive, and inkjet-printable graphene-based inks, Adv. Funct. Mater. 32 (2) (2022) 2105028, https://doi.org/10.1002/adfm.202105028.

[61] F. Schedin, A.K. Geim, S.V. Morozov, E.W. Hill, P. Blake, M.I. Katsnelson, K. S. Novoselov, Detection of individual gas molecules adsorbed on graphene, Nat. Mater. 6 (9) (2007) 652–655, https://doi.org/10.1038/nmat1967.

[62] W. Yan, H.-R. Fuh, Y. Lv, K.-Q. Chen, T.-Y. Tsai, Y.-R. Wu, T.-H. Shieh, K.-M. Hung, J. Li, D. Zhang, C.Ó. Coileáin, S.K. Arora, Z. Wang, Z. Jiang, C.-R. Chang, H.-C. Wu, Giant gauge factor of Van der Waals material based strain sensors, Nat. Commun. 12 (1) (2021) 2018, https://doi.org/10.1038/s41467-021-22316-8.

[63] J. Wan, S.D. Lacey, J. Dai, W. Bao, M.S. Fuhrer, L. Hu, Tuning two-dimensional nanomaterials by intercalation: materials, properties and applications, Chem. Soc. Rev. 45 (24) (2016) 6742–6765, https://doi.org/10.1039/C5CS00758E.

[64] H.L. Chia, C.C. Mayorga-Martinez, M. Pumera, Doping and decorating 2D materials for biosensing: benefits and drawbacks, Adv. Funct. Mater. 31 (46) (2021) 2102555, https://doi.org/10.1002/adfm.202102555.

[65] Z. Li, S.L. Wong, Functionalization of 2D transition metal dichalcogenides for biomedical applications, Mater. Sci. Eng. C 70 (2017) 1095–1106, https://doi.org/10.1016/j.msec.2016.03.039.

[66] Y. Xu, X. Xie, R. Zhang, W. Yuan, Functionalization of black phosphorus nanosheets via self-polymerization of dopamine and subsequent secondary reactions for gas sensing investigation, Sensors Actuators B Chem. 372 (2022), 132670, https://doi.org/10.1016/j.snb.2022.132670.

[67] L. Daukiya, J. Seibel, S. De Feyter, Chemical modification of 2D materials using molecules and assemblies of molecules, Adv. Phys. X 4 (1) (2019) 1625723, https://doi.org/10.1080/23746149.2019.1625723.

[68] M. Gobbi, E. Orgiu, P. Samorì, When 2D materials meet molecules: Opportunities and challenges of hybrid organic/inorganic Van Der Waals heterostructures, Adv. Mater. 30 (18) (2018) 1706103, https://doi.org/10.1002/adma.201706103.

[69] S. Eissa, G.C. Jimenez, F. Mahvash, A. Guermoune, C. Tlili, T. Szkopek, M. Zourob, M. Siaj, Functionalized CVD monolayer graphene for label-free impedimetric biosensing, Nano Res. 8 (5) (2015) 1698–1709, https://doi.org/10.1007/s12274-014-0671-0.

[70] F. Khurshid, M. Jeyavelan, K. Takahashi, M.S. Leo Hudson, S. Nagarajan, Aryl fluoride functionalized graphene oxides for excellent room temperature ammonia sensitivity/selectivity, RSC Adv. 8 (36) (2018) 20440–20449, https://doi.org/10.1039/C8RA01818A.

[71] M. Qi, Y. Zhang, C. Cao, M. Zhang, S. Liu, G. Liu, Decoration of reduced graphene oxide nanosheets with aryldiazonium salts and gold nanoparticles toward a label-free amperometric immunosensor for detecting cytokine tumor necrosis factor-α in live cells, Anal. Chem. 88 (19) (2016) 9614–9621, https://doi.org/10.1021/acs.analchem.6b02353.

[72] M.N. Islam, R.B. Channon, Chapter 1.3 - Electrochemical sensors, in: S. Ladame, J.Y.H. Chang (Eds.), Bioengineering Innovative Solutions for Cancer, Academic Press, 2020, pp. 47–71, https://doi.org/10.1016/B978-0-12-813886-1.00004-8.

[73] C.W. Lee, J.M. Suh, H.W. Jang, Chemical sensors based on two-dimensional (2D) materials for selective detection of ions and molecules in liquid, Front. Chem. 7 (2019).

[74] A. Chowdhury, S. Biswas, T. Singh, A. Chandra, Redox mediator induced electrochemical reactions at the electrode-electrolyte interface: making sodium-

ion supercapacitors a competitive technology, Electroch. Sci. Adv. 2 (1) (2022), e2100030, https://doi.org/10.1002/elsa.202100030.
[75] M. Labib, E.H. Sargent, S.O. Kelley, Electrochemical methods for the analysis of clinically relevant biomolecules, Chem. Rev. 116 (16) (2016) 9001–9090, https://doi.org/10.1021/acs.chemrev.6b00220.
[76] D.R. Thévenot, K. Toth, R.A. Durst, G.S. Wilson, Electrochemical biosensors: recommended definitions and classification1International Union of Pure and Applied Chemistry: Physical Chemistry Division, Commission I.7 (Biophysical Chemistry); Analytical Chemistry Division, Commission V.5 (Electroanalytical Chemistry).1, Biosens. Bioelectron. 16 (1) (2001) 121–131, https://doi.org/10.1016/S0956-5663(01)00115-4.
[77] F. Scholz, Voltammetric techniques of analysis: the essentials, ChemTexts 1 (4) (2015) 17, https://doi.org/10.1007/s40828-015-0016-y.
[78] Q. He, H.G. Sudibya, Z. Yin, S. Wu, H. Li, F. Boey, W. Huang, P. Chen, H. Zhang, Centimeter-long and large-scale micropatterns of reduced graphene oxide films: fabrication and sensing applications, ACS Nano 4 (6) (2010) 3201–3208, https://doi.org/10.1021/nn100780v.
[79] J. Kudr, V. Adam, O. Zitka, Fabrication of graphene/molybdenum disulfide composites and their usage as actuators for electrochemical sensors and biosensors, Molecules 24 (18) (2019) 3374.
[80] S.N. Kajale, S. Yadav, Y. Cai, B. Joy, D. Sarkar, 2D material based field effect transistors and nanoelectromechanical systems for sensing applications, iScience 24 (12) (2021), https://doi.org/10.1016/j.isci.2021.103513.
[81] R. Vargas-Bernal, Electrical properties of two-dimensional materials used in gas sensors, Sensors (2019), https://doi.org/10.3390/s19061295.
[82] P. Zhang, Y. Xiao, J. Zhang, B. Liu, X. Ma, Y. Wang, Highly sensitive gas sensing platforms based on field effect Transistor-a review, Anal. Chim. Acta 1172 (2021), 338575, https://doi.org/10.1016/j.aca.2021.338575.
[83] W. Hu, Z. Sheng, X. Hou, H. Chen, Z. Zhang, D.W. Zhang, P. Zhou, Ambipolar 2D semiconductors and emerging device applications, Small Methods 5 (1) (2021) 2000837, https://doi.org/10.1002/smtd.202000837.
[84] C. Dai, Y. Liu, D. Wei, Two-dimensional field-effect transistor sensors: the road toward commercialization, Chem. Rev. 122 (11) (2022) 10319–10392, https://doi.org/10.1021/acs.chemrev.1c00924.
[85] H. Hashtroudi, I.D.R. Mackinnon, M. Shafiei, Emerging 2D hybrid nanomaterials: towards enhanced sensitive and selective conductometric gas sensors at room temperature, J. Mater. Chem. C 8 (38) (2020) 13108–13126, https://doi.org/10.1039/D0TC01968B.
[86] Y. Wang, Y. Zhou, Y. Wang, R. Zhang, J. Li, X. Li, Z. Zang, Conductometric room temperature ammonia sensors based on titanium dioxide nanoparticles decorated thin black phosphorus nanosheets, Sensors Actuators B Chem. 349 (2021), 130770, https://doi.org/10.1016/j.snb.2021.130770.
[87] F.S. Irani, A.H. Shafaghi, M.C. Tasdelen, T. Delipinar, C.E. Kaya, G.G. Yapici, M. K. Yapici, Graphene as a piezoresistive material in strain sensing applications, Micromachines (2022), https://doi.org/10.3390/mi13010119.
[88] L. Zheng, X. Wang, H. Jiang, M. Xu, W. Huang, Z. Liu, Recent progress of flexible electronics by 2D transition metal dichalcogenides, Nano Res. 15 (3) (2022) 2413–2432, https://doi.org/10.1007/s12274-021-3779-z.
[89] A. Dominguez-Alfaro, I.J. Gómez, N. Alegret, D. Mecerreyes, M. Prato, 2D and 3D immobilization of carbon nanomaterials into PEDOT via electropolymerization of a functional Bis-EDOT monomer, Polymers (2021), https://doi.org/10.3390/polym13030436.
[90] Z.-L. Lei, B. Guo, 2D material-based optical biosensor: status and prospect, Adv. Sci. 9 (4) (2022) 2102924, https://doi.org/10.1002/advs.202102924.
[91] Q. Duan, Y. Liu, S. Chang, H. Chen, J.-H. Chen, Surface plasmonic sensors: sensing mechanism and recent applications, Sensors (2021), https://doi.org/10.3390/s21165262.
[92] B.B. Subbanna, K. Choudhary, S. Singh, S. Kumar, 2D material-based optical sensors: a review, ISSS J. Micro Smart Syst. 11 (1) (2022) 169–177, https://doi.org/10.1007/s41683-021-00083-4.
[93] X. Luo, T. Qiu, W. Lu, Z. Ni, Plasmons in graphene: recent progress and applications, Mater. Sci. Eng. R. Rep. 74 (11) (2013) 351–376, https://doi.org/10.1016/j.mser.2013.09.001.
[94] J. Zhou, T. Yang, J. Chen, C. Wang, H. Zhang, Y. Shao, Two-dimensional nanomaterial-based plasmonic sensing applications: advances and challenges, Coord. Chem. Rev. 410 (2020), 213218, https://doi.org/10.1016/j.ccr.2020.213218.
[95] Y. Ge, S. Chen, Y. Xu, Z. He, Z. Liang, Y. Chen, Y. Song, D. Fan, K. Zhang, H. Zhang, Few-layer selenium-doped black phosphorus: synthesis, nonlinear optical properties and ultrafast photonics applications, J. Mater. Chem. C 5 (25) (2017) 6129–6135, https://doi.org/10.1039/C7TC01267E.
[96] W. Wang, W. Wang, L. Liu, L. Xu, H. Kuang, J. Zhu, C. Xu, Nanoshell-enhanced Raman spectroscopy on a microplate for staphylococcal Enterotoxin B sensing, ACS Appl. Mater. Interfaces 8 (24) (2016) 15591–15597, https://doi.org/10.1021/acsami.6b02905.
[97] X.M. Qian, S.M. Nie, Single-molecule and single-nanoparticle SERS: from fundamental mechanisms to biomedical applications, Chem. Soc. Rev. 37 (5) (2008) 912–920, https://doi.org/10.1039/B708839F.
[98] W. Ji, X. Xue, W. Ruan, C. Wang, N. Ji, L. Chen, Z. Li, W. Song, B. Zhao, J. R. Lombardi, Scanned chemical enhancement of surface-enhanced Raman scattering using a charge-transfer complex, Chem. Commun. 47 (8) (2011) 2426–2428, https://doi.org/10.1039/C0CC03697H.
[99] M. Chen, D. Liu, X. Du, K.H. Lo, S. Wang, B. Zhou, H. Pan, 2D materials: excellent substrates for surface-enhanced Raman scattering (SERS) in chemical sensing and biosensing, TrAC Trends Anal. Chem. 130 (2020), 115983, https://doi.org/10.1016/j.trac.2020.115983.
[100] M. Devi, Application of 2D Nanomaterials as Fluorescent Biosensors, Adapting 2D Nanomaterials for Advanced Applications, American Chemical Society, 2020, pp. 117–141, https://doi.org/10.1021/bk-2020-1353.ch006.
[101] P.M. Neema, A.M. Tomy, J. Cyriac, Chemical sensor platforms based on fluorescence resonance energy transfer (FRET) and 2D materials, TrAC Trends Anal. Chem. 124 (2020), 115797, https://doi.org/10.1016/j.trac.2019.115797.
[102] G.A. Jones, D.S. Bradshaw, Resonance energy transfer: from fundamental theory to recent applications, Front. Phys. 7 (2019).
[103] F. Tian, J. Lyu, J. Shi, M. Yang, Graphene and graphene-like two-denominational materials based fluorescence resonance energy transfer (FRET) assays for biological applications, Biosens. Bioelectron. 89 (2017) 123–135, https://doi.org/10.1016/j.bios.2016.06.046.
[104] L. Yan, H. Shi, X. Sui, Z. Deng, L. Gao, MoS_2-DNA and MoS_2 based sensors, RSC Adv. 7 (38) (2017) 23573–23582, https://doi.org/10.1039/C7RA02649H.
[105] J. Zhou, Z. Li, M. Ying, M. Liu, X. Wang, X. Wang, L. Cao, H. Zhang, G. Xu, Black phosphorus nanosheets for rapid microRNA detection, Nanoscale 10 (11) (2018) 5060–5064, https://doi.org/10.1039/C7NR08900G.
[106] J. Zhou, J. Chen, Y. Ge, Y. Shao, Two-dimensional nanomaterials for Förster resonance energy transfer–based sensing applications 9 (7) (2020) 1855–1875, https://doi.org/10.1515/nanoph-2020-0065.
[107] J. Dai, O. Ogbeide, N. Macadam, Q. Sun, W. Yu, Y. Li, B.-L. Su, T. Hasan, X. Huang, W. Huang, Printed gas sensors, Chem. Soc. Rev. 49 (6) (2020) 1756–1789, https://doi.org/10.1039/C9CS00459A.
[108] R.K. Jha, N. Bhat, Recent progress in chemiresistive gas sensing technology based on molybdenum and tungsten chalcogenide nanostructures, Adv. Mater. Interfaces 7 (7) (2020) 1901992, https://doi.org/10.1002/admi.201901992.
[109] C. Anichini, W. Czepa, D. Pakulski, A. Aliprandi, A. Ciesielski, P. Samorì, Chemical sensing with 2D materials, Chem. Soc. Rev. 47 (13) (2018) 4860–4908, https://doi.org/10.1039/C8CS00417J.
[110] Z. Feng, Y. Xie, J. Chen, Y. Yu, S. Zheng, R. Zhang, Q. Li, X. Chen, C. Sun, H. Zhang, W. Pang, J. Liu, D. Zhang, Highly sensitive $MoTe_2$ chemical sensor with fast recovery rate through gate biasing, 2D, Materials 4 (2) (2017), 025018, https://doi.org/10.1088/2053-1583/aa57fe.
[111] N. Huo, S. Yang, Z. Wei, S.-S. Li, J.-B. Xia, J. Li, Photoresponsive and gas sensing field-effect transistors based on multilayer WS_2 nanoflakes, Sci. Rep. 4 (1) (2014) 5209, https://doi.org/10.1038/srep05209.
[112] J. Baek, D. Yin, N. Liu, I. Omkaram, C. Jung, H. Im, S. Hong, S.M. Kim, Y.K. Hong, J. Hur, Y. Yoon, S. Kim, A highly sensitive chemical gas detecting transistor based on highly crystalline CVD-grown $MoSe_2$ films, Nano Res. 10 (6) (2017) 1861–1871, https://doi.org/10.1007/s12274-016-1291-7.
[113] S. Guo, D. Yang, S. Zhang, Q. Dong, B. Li, N. Tran, Z. Li, Y. Xiong, M.E. Zaghloul, Development of a cloud-based epidermal $MoSe_2$ device for hazardous gas sensing, Adv. Funct. Mater. 29 (18) (2019) 1900138, https://doi.org/10.1002/adfm.201900138.
[114] Y. Hong, W.-M. Kang, I.-T. Cho, J. Shin, M. Wu, J.-H. Lee, Gas-sensing characteristics of exfoliated WSe_2 field-effect transistors, J. Nanosci. Nanotechnol. 17 (5) (2017) 3151–3154.
[115] M. Donarelli, S. Prezioso, F. Perrozzi, F. Bisti, M. Nardone, L. Giancaterini, C. Cantalini, L. Ottaviano, Response to NO_2 and other gases of resistive chemically exfoliated MoS_2-based gas sensors, Sensors Actuators B Chem. 207 (2015) 602–613, https://doi.org/10.1016/j.snb.2014.10.099.
[116] C. Zhou, W. Yang, H. Zhu, Mechanism of charge transfer and its impacts on Fermi-level pinning for gas molecules adsorbed on monolayer WS_2, J. Chem. Phys. 142 (21) (2015), 214704, https://doi.org/10.1063/1.4922049.
[117] D. Matatagui, C. Cruz, F. Carrascoso, A.M. Al-Enizi, A. Nafady, A. Castellanos-Gomez, M.D. Horrillo, Eco-friendly disposable WS_2 paper sensor for sub-ppm NO_2 detection at room temperature, Nanomaterials (2022), https://doi.org/10.3390/nano12071213.
[118] R.K. Jha, P.K. Guha, Liquid exfoliated pristine WS_2 nanosheets for ultrasensitive and highly stable chemiresistive humidity sensors, Nanotechnology 27 (47) (2016), 475503, https://doi.org/10.1088/0957-4484/27/47/475503.
[119] X. Li, X. Li, Z. Li, J. Wang, J. Zhang, WS_2 nanoflakes based selective ammonia sensors at room temperature, Sensors Actuators B Chem. 240 (2017) 273–277, https://doi.org/10.1016/j.snb.2016.08.163.
[120] M. O'Brien, K. Lee, R. Morrish, N.C. Berner, N. McEvoy, C.A. Wolden, G. S. Duesberg, Plasma assisted synthesis of WS_2 for gas sensing applications, Chem. Phys. Lett. 615 (2014) 6–10, https://doi.org/10.1016/j.cplett.2014.09.051.
[121] T. Xu, Y. Liu, Y. Pei, Y. Chen, Z. Jiang, Z. Shi, J. Xu, D. Wu, Y. Tian, X. Li, The ultra-high NO2 response of ultra-thin WS_2 nanosheets synthesized by hydrothermal and calcination processes, Sensors Actuators B Chem. 259 (2018) 789–796, https://doi.org/10.1016/j.snb.2017.12.070.
[122] R. Guo, Y. Han, C. Su, X. Chen, M. Zeng, N. Hu, Y. Su, Z. Zhou, H. Wei, Z. Yang, Ultrasensitive room temperature NO_2 sensors based on liquid phase exfoliated WSe_2 nanosheets, Sensors Actuators B Chem. 300 (2019), 127013, https://doi.org/10.1016/j.snb.2019.127013.
[123] F.K. Perkins, A.L. Friedman, E. Cobas, P.M. Campbell, G.G. Jernigan, B.T. Jonker, Chemical vapor sensing with monolayer MoS_2, Nano Lett. 13 (2) (2013) 668–673, https://doi.org/10.1021/nl3043079.
[124] B. Cho, M.G. Hahm, M. Choi, J. Yoon, A.R. Kim, Y.-J. Lee, S.-G. Park, J.-D. Kwon, C.S. Kim, M. Song, Y. Jeong, K.-S. Nam, S. Lee, T.J. Yoo, C.G. Kang, B.H. Lee, H. C. Ko, P.M. Ajayan, D.-H. Kim, Charge-transfer-based gas sensing using atomic-layer MoS_2, Sci. Rep. 5 (1) (2015) 8052, https://doi.org/10.1038/srep08052.
[125] Y. Zhao, J.-G. Song, G.H. Ryu, K.Y. Ko, W.J. Woo, Y. Kim, D. Kim, J.H. Lim, S. Lee, Z. Lee, J. Park, H. Kim, Low-temperature synthesis of 2D MoS_2 on a plastic substrate for a flexible gas sensor, Nanoscale 10 (19) (2018) 9338–9345, https://doi.org/10.1039/C8NR00108A.

[126] S.-Y. Cho, S.J. Kim, Y. Lee, J.-S. Kim, W.-B. Jung, H.-W. Yoo, J. Kim, H.-T. Jung, Highly enhanced gas adsorption properties in vertically aligned MoS_2 layers, ACS Nano 9 (9) (2015) 9314–9321, https://doi.org/10.1021/acsnano.5b04504.
[127] Y.-Z. Chen, S.-W. Wang, C.-C. Yang, C.-H. Chung, Y.-C. Wang, S.-W. Huang Chen, C.-W. Chen, T.-Y. Su, H.-N. Lin, H.-C. Kuo, Y.-L. Chueh, An indoor light-activated 3D cone-shaped MoS_2 bilayer-based NO gas sensor with PPb-level detection at room-temperature, Nanoscale 11 (21) (2019) 10410–10419, https://doi.org/10.1039/C8NR10157D.
[128] D.J. Late, T. Doneux, M. Bougouma, Single-layer $MoSe_2$ based NH_3 gas sensor, Appl. Phys. Lett. 105 (23) (2014), 233103, https://doi.org/10.1063/1.4903358.
[129] R.K. Jha, J.V. D'Costa, N. Sakhuja, N. Bhat, $MoSe_2$ nanoflakes based chemiresistive sensors for ppb-level hydrogen sulfide gas detection, Sensors Actuators B Chem. 297 (2019), 126687, https://doi.org/10.1016/j.snb.2019.126687.
[130] S.Y. Choi, Y. Kim, H.-S. Chung, A.R. Kim, J.-D. Kwon, J. Park, Y.L. Kim, S.-H. Kwon, M.G. Hahm, B. Cho, Effect of Nb doping on chemical sensing performance of two-dimensional layered $MoSe_2$, ACS Appl. Mater. Interfaces 9 (4) (2017) 3817–3823, https://doi.org/10.1021/acsami.6b14551.
[131] E. Wu, Y. Xie, B. Yuan, H. Zhang, X. Hu, J. Liu, D. Zhang, Ultrasensitive and fully reversible NO2 gas sensing based on p-Type $MoTe_2$ under ultraviolet illumination, ACS Sens. 3 (9) (2018) 1719–1726, https://doi.org/10.1021/acssensors.8b00461.
[132] H. Tabata, H. Matsuyama, T. Goto, O. Kubo, M. Katayama, Visible-light-activated response originating from carrier-mobility modulation of NO_2 gas sensors based on MoS_2 monolayers, ACS Nano 15 (2) (2021) 2542–2553, https://doi.org/10.1021/acsnano.0c06996.
[133] J. Hu, J. Zhang, Z. Zhao, J. Liu, J. Shi, G. Li, P. Li, W. Zhang, K. Lian, S. Zhuiykov, Synthesis and electrochemical properties of rGO-MoS_2 heterostructures for highly sensitive nitrite detection, Ionics 24 (2) (2018) 577–587, https://doi.org/10.1007/s11581-017-2202-y.
[134] C. Gautam, C.S. Tiwary, L.D. Machado, S. Jose, S. Ozden, S. Biradar, D.S. Galvao, R.K. Sonker, B.C. Yadav, R. Vajtai, P.M. Ajayan, Synthesis and porous h-BN 3D architectures for effective humidity and gas sensors, RSC Adv. 6 (91) (2016) 87888–87896, https://doi.org/10.1039/C6RA18833H.
[135] N. Goel, M. Kumar, Recent advances in ultrathin 2D hexagonal boron nitride based gas sensors, J. Mater. Chem. C 9 (5) (2021) 1537–1549, https://doi.org/10.1039/D0TC05855F.
[136] L. Lin, T. Liu, Y. Zhang, R. Sun, W. Zeng, Z. Wang, Synthesis of boron nitride nanosheets with a few atomic layers and their gas-sensing performance, Ceram. Int. 42 (1, Part A) (2016) 971–975, https://doi.org/10.1016/j.ceramint.2015.08.109.
[137] S.J. Kim, H.-J. Koh, C.E. Ren, O. Kwon, K. Maleski, S.-Y. Cho, B. Anasori, C.-K. Kim, Y.-K. Choi, J. Kim, Y. Gogotsi, H.-T. Jung, Metallic $Ti_3C_2T_x$ MXene gas sensors with ultrahigh signal-to-noise ratio, ACS Nano 12 (2) (2018) 986–993, https://doi.org/10.1021/acsnano.7b07460.
[138] W. Yuan, K. Yang, H. Peng, F. Li, F. Yin, A flexible VOCs sensor based on a 3D Mxene framework with a high sensing performance, J. Mater. Chem. A 6 (37) (2018) 18116–18124, https://doi.org/10.1039/C8TA06928J.
[139] G. Lu, H. Li, C. Liusman, Z. Yin, S. Wu, H. Zhang, Surface enhanced Raman scattering of Ag or Au nanoparticle-decorated reduced graphene oxide for detection of aromatic molecules, Chem. Sci. 2 (9) (2011) 1817–1821, https://doi.org/10.1039/C1SC00254F.
[140] C. Hu, J. Rong, J. Cui, Y. Yang, L. Yang, Y. Wang, Y. Liu, Fabrication of a graphene oxide–gold nanorod hybrid material by electrostatic self-assembly for surface-enhanced Raman scattering, Carbon 51 (2013) 255–264, https://doi.org/10.1016/j.carbon.2012.08.051.
[141] E. Er, A. Sánchez-Iglesias, A. Silvestri, B. Arnaiz, L.M. Liz-Marzán, M. Prato, A. Criado, Metal nanoparticles/MoS_2 surface-enhanced raman scattering-based sandwich immunoassay for α-fetoprotein detection, ACS Appl. Mater. Interfaces 13 (7) (2021) 8823–8831, https://doi.org/10.1021/acsami.0c22203.
[142] S. Su, C. Zhang, L. Yuwen, J. Chao, X. Zuo, X. Liu, C. Song, C. Fan, L. Wang, Creating SERS hot spots on MoS_2 nanosheets with in situ grown gold nanoparticles, ACS Appl. Mater. Interfaces 6 (21) (2014) 18735–18741, https://doi.org/10.1021/am5043092.
[143] E. Satheeshkumar, T. Makaryan, A. Melikyan, H. Minassian, Y. Gogotsi, M. Yoshimura, One-step solution processing of Ag, Au and Pd@MXene hybrids for SERS, Sci. Rep. 6 (1) (2016) 32049, https://doi.org/10.1038/srep32049.
[144] S. Zhang, D. Zhang, X. Zhang, D. Shang, Z. Xue, D. Shan, X. Lu, Ultratrace naked-eye colorimetric detection of Hg^{2+} in wastewater and serum utilizing mercury-stimulated peroxidase mimetic activity of reduced graphene oxide-PEI-Pd nanohybrids, Anal. Chem. 89 (6) (2017) 3538–3544, https://doi.org/10.1021/acs.analchem.6b04805.
[145] Y. Wang, S. Wang, N. Dong, W. Kang, K. Li, Z. Nie, Titanium carbide mxenes mediated in situ reduction allows label-free and visualized nanoplasmonic sensing of silver ions, Anal. Chem. 92 (6) (2020) 4623–4629, https://doi.org/10.1021/acs.analchem.0c00164.
[146] S.R. Tamalampudi, Y.-Y. Lu, R.K. U, R. Sankar, C.-D. Liao, K.M. B, C.-H. Cheng, F. C. Chou, Y.-T. Chen, High performance and bendable few-layered inse photodetectors with broad spectral response, Nano Lett. 14 (5) (2014) 2800–2806, https://doi.org/10.1021/nl500817g.
[147] J. Quereda, S. Kuriakose, C. Munuera, F.J. Mompean, A.M. Al-Enizi, A. Nafady, E. Diez, R. Frisenda, A. Castellanos-Gomez, Scalable and low-cost fabrication of flexible WS_2 photodetectors on polycarbonate, npj Flexible, Electronics 6 (1) (2022) 23, https://doi.org/10.1038/s41528-022-00157-9.
[148] W. Zhang, Q. Zhao, C. Munuera, M. Lee, E. Flores, J.E.F. Rodrigues, J.R. Ares, C. Sanchez, J. Gainza, H.S.J. van der Zant, J.A. Alonso, I.J. Ferrer, T. Wang, R. Frisenda, A. Castellanos-Gomez, Integrating van der Waals materials on paper substrates for electrical and optical applications, Appl. Mater. Today 23 (2021), 101012, https://doi.org/10.1016/j.apmt.2021.101012.
[149] I. Hwang, J.S. Kim, S.H. Cho, B. Jeong, C. Park, Flexible vertical p–n diode photodetectors with thin N-type $MoSe_2$ films solution-processed on water surfaces, ACS Appl. Mater. Interfaces 10 (40) (2018) 34543–34552, https://doi.org/10.1021/acsami.8b07279.
[150] S.-H. Bae, Y. Lee, B.K. Sharma, H.-J. Lee, J.-H. Kim, J.-H. Ahn, Graphene-based transparent strain sensor, Carbon 51 (2013) 236–242, https://doi.org/10.1016/j.carbon.2012.08.048.
[151] Y. Wang, R. Yang, Z. Shi, L. Zhang, D. Shi, E. Wang, G. Zhang, Super-elastic graphene ripples for flexible strain sensors, ACS Nano 5 (5) (2011) 3645–3650, https://doi.org/10.1021/nn103523t.
[152] Z. Ismail, Application of Clean & Clear ® polymer film as a substrate for flexible and highly sensitive graphene–based strain sensor, Org. Electron. 77 (2020), 105501, https://doi.org/10.1016/j.orgel.2019.105501.
[153] T. Gong, H. Zhang, W. Huang, L. Mao, Y. Ke, M. Gao, B. Yu, Highly responsive flexible strain sensor using polystyrene nanoparticle doped reduced graphene oxide for human health monitoring, Carbon 140 (2018) 286–295, https://doi.org/10.1016/j.carbon.2018.09.007.
[154] X. Wang, Y. Qiu, W. Cao, P. Hu, Highly stretchable and conductive core–sheath chemical vapor deposition graphene fibers and their applications in safe strain sensors, Chem. Mater. 27 (20) (2015) 6969–6975, https://doi.org/10.1021/acs.chemmater.5b02098.
[155] S. Chen, Y. Wei, S. Wei, Y. Lin, L. Liu, Ultrasensitive cracking-assisted strain sensors based on silver nanowires/graphene hybrid particles, ACS Appl. Mater. Interfaces 8 (38) (2016) 25563–25570, https://doi.org/10.1021/acsami.6b09188.
[156] M. Park, Y.J. Park, X. Chen, Y.-K. Park, M.-S. Kim, J.-H. Ahn, MoS_2-based tactile sensor for electronic skin applications, Adv. Mater. 28 (13) (2016) 2556–2562, https://doi.org/10.1002/adma.201505124.
[157] Y.J. Park, B.K. Sharma, S.M. Shinde, M.-S. Kim, B. Jang, J.-H. Kim, J.-H. Ahn, All MoS_2-based large area, skin-attachable active-matrix tactile sensor, ACS Nano 13 (3) (2019) 3023–3030, https://doi.org/10.1021/acsnano.8b07995.
[158] S. Zhang, Y. Song, M. Wang, G. Xiao, F. Gao, Z. Li, G. Tao, P. Zhuang, F. Yue, P. Chan, X. Cai, Real-time simultaneous recording of electrophysiological activities and dopamine overflow in the deep brain nuclei of a non-human primate with Parkinson's disease using nano-based microelectrode arrays, Microsyst. Nanoeng. 4 (1) (2018) 17070, https://doi.org/10.1038/micronano.2017.70.
[159] V.K. Sangwan, M.C. Hersam, Neuromorphic nanoelectronic materials, Nat. Nanotechnol. 15 (7) (2020) 517–528, https://doi.org/10.1038/s41565-020-0647-z.
[160] C. Schmidt, Bioelectronics: the bionic material, Nature 483 (7389) (2012) S37, https://doi.org/10.1038/483S37a.
[161] N. Rohaizad, C.C. Mayorga-Martinez, M. Fojtů, N.M. Latiff, M. Pumera, Two-dimensional materials in biomedical, biosensing and sensing applications, Chem. Soc. Rev. 50 (1) (2021) 619–657, https://doi.org/10.1039/D0CS00150C.
[162] J. Park, J. Kim, S.-Y. Kim, W.H. Cheong, J. Jang, Y.-G. Park, K. Na, Y.-T. Kim, J. H. Heo, C.Y. Lee, J.H. Lee, F. Bien, J.-U. Park, Soft, smart contact lenses with integrations of wireless circuits, glucose sensors, and displays, Science, Advances 4 (1) (2018) eaap9841, https://doi.org/10.1126/sciadv.aap9841.
[163] H. Lee, Y. Lee, C. Song, H.R. Cho, R. Ghaffari, T.K. Choi, K.H. Kim, Y.B. Lee, D. Ling, H. Lee, S.J. Yu, S.H. Choi, T. Hyeon, D.-H. Kim, An endoscope with integrated transparent bioelectronics and theranostic nanoparticles for colon cancer treatment, Nat. Commun. 6 (1) (2015) 10059, https://doi.org/10.1038/ncomms10059.
[164] A. Silvestri, C. Wetzl, N. Alegret, L. Cardo, H.-L. Hou, A. Criado, M. Prato, The era of nano-bionic: 2D materials for wearable and implantable body sensors, Adv. Drug Deliv. Rev. 186 (2022), 114315, https://doi.org/10.1016/j.addr.2022.114315.
[165] J. Jang, J. Kim, H. Shin, Y.-G. Park, B.J. Joo, H. Seo, J.-E. Won, D.W. Kim, C. Y. Lee, H.K. Kim, J.-U. Park, Smart contact lens and transparent heat patch for remote monitoring and therapy of chronic ocular surface inflammation using mobiles, Science Advances 7 (14) (2021) eabf7194, https://doi.org/10.1126/sciadv.abf7194.
[166] J. Kim, M. Kim, M.-S. Lee, K. Kim, S. Ji, Y.-T. Kim, J. Park, K. Na, K.-H. Bae, H. Kyun Kim, F. Bien, C. Young Lee, J.-U. Park, Wearable smart sensor systems integrated on soft contact lenses for wireless ocular diagnostics, Nat. Commun. 8 (1) (2017) 14997, https://doi.org/10.1038/ncomms14997.
[167] G. Rong, S.R. Corrie, H.A. Clark, In vivo biosensing: progress and perspectives, ACS Sens. 2 (3) (2017) 327–338, https://doi.org/10.1021/acssensors.6b00834.
[168] P. Suvarnaphaet, S. Pechprasarn, Graphene-based materials for biosensors: a review, Sensors (2017), https://doi.org/10.3390/s17102161.
[169] G. Reina, J.M. González-Domínguez, A. Criado, E. Vázquez, A. Bianco, M. Prato, Promises, facts and challenges for graphene in biomedical applications, Chem. Soc. Rev. 46 (15) (2017) 4400–4416, https://doi.org/10.1039/C7CS00363C.
[170] A. Ambrosi, C.K. Chua, N.M. Latiff, A.H. Loo, C.H.A. Wong, A.Y.S. Eng, A. Bonanni, M. Pumera, Graphene and its electrochemistry – an update, Chem. Soc. Rev. 45 (9) (2016) 2458–2493, https://doi.org/10.1039/C6CS00136J.
[171] J. Kim, Y. Lee, M. Kang, L. Hu, S. Zhao, J.-H. Ahn, 2D materials for skin-mountable electronic devices, Adv. Mater. 33 (47) (2021) 2005858, https://doi.org/10.1002/adma.202005858.
[172] V. Georgakilas, J.N. Tiwari, K.C. Kemp, J.A. Perman, A.B. Bourlinos, K.S. Kim, R. Zboril, Noncovalent functionalization of graphene and graphene oxide for

energy materials, biosensing, catalytic, and biomedical applications, Chem. Rev. 116 (9) (2016) 5464–5519, https://doi.org/10.1021/acs.chemrev.5b00620.
[173] R.M. Torrente-Rodríguez, J. Tu, Y. Yang, J. Min, M. Wang, Y. Song, Y. Yu, C. Xu, C. Ye, W.W. IsHak, W. Gao, Investigation of cortisol dynamics in human sweat using a graphene-based wireless mhealth system, Matter 2 (4) (2020) 921–937, https://doi.org/10.1016/j.matt.2020.01.021.
[174] Z. Wang, J. Shin, J.-H. Park, H. Lee, D.-H. Kim, H. Liu, Engineering materials for electrochemical sweat sensing, Adv. Funct. Mater. 31 (12) (2021) 2008130, https://doi.org/10.1002/adfm.202008130.
[175] Y.J. Yun, J. Ju, J.H. Lee, S.-H. Moon, S.-J. Park, Y.H. Kim, W.G. Hong, D.H. Ha, H. Jang, G.H. Lee, H.-M. Chung, J. Choi, S.W. Nam, S.-H. Lee, Y. Jun, Highly elastic graphene-based electronics toward electronic skin, Adv. Funct. Mater. 27 (33) (2017) 1701513, https://doi.org/10.1002/adfm.201701513.
[176] Y. Lei, W. Zhao, Y. Zhang, Q. Jiang, J.-H. He, A.J. Baeumner, O.S. Wolfbeis, Z. L. Wang, K.N. Salama, H.N. Alshareef, A MXene-based wearable biosensor system for high-performance in vitro perspiration analysis, Small 15 (19) (2019) 1901190, https://doi.org/10.1002/smll.201901190.
[177] G. Li, D. Wen, Sensing nanomaterials of wearable glucose sensors, Chin. Chem. Lett. 32 (1) (2021) 221–228, https://doi.org/10.1016/j.cclet.2020.10.028.
[178] H. Lee, T.K. Choi, Y.B. Lee, H.R. Cho, R. Ghaffari, L. Wang, H.J. Choi, T.D. Chung, N. Lu, T. Hyeon, S.H. Choi, D.-H. Kim, A graphene-based electrochemical device with thermoresponsive microneedles for diabetes monitoring and therapy, Nat. Nanotechnol. 11 (6) (2016) 566–572, https://doi.org/10.1038/nnano.2016.38.
[179] L. Lorencova, T. Bertok, J. Filip, M. Jerigova, D. Velic, P. Kasak, K.A. Mahmoud, J. Tkac, Highly stable $Ti_3C_2T_x$ (MXene)/Pt nanoparticles-modified glassy carbon electrode for H2O2 and small molecules sensing applications, Sensors Actuators B Chem. 263 (2018) 360–368, https://doi.org/10.1016/j.snb.2018.02.124.
[180] Z. Hao, Y. Luo, C. Huang, Z. Wang, G. Song, Y. Pan, X. Zhao, S. Liu, An intelligent graphene-based biosensing device for cytokine storm syndrome biomarkers detection in human biofluids, Small 17 (29) (2021) 2101508, https://doi.org/10.1002/smll.202101508.
[181] Y. Lei, D. Butler, M.C. Lucking, F. Zhang, T. Xia, K. Fujisawa, T. Granzier-Nakajima, R. Cruz-Silva, M. Endo, H. Terrones, M. Terrones, A. Ebrahimi, Single-atom doping of MoS_2 with manganese enables ultrasensitive detection of dopamine: Experimental and computational approach, Sci. Adv. 6 (32) (2020) eabc4250, https://doi.org/10.1126/sciadv.abc4250.
[182] R. Goldoni, M. Farronato, S.T. Connelly, G.M. Tartaglia, W.-H. Yeo, Recent advances in graphene-based nanobiosensors for salivary biomarker detection, Biosens. Bioelectron. 171 (2021), 112723, https://doi.org/10.1016/j.bios.2020.112723.
[183] M.S. Mannoor, H. Tao, J.D. Clayton, A. Sengupta, D.L. Kaplan, R.R. Naik, N. Verma, F.G. Omenetto, M.C. McAlpine, Graphene-based wireless bacteria detection on tooth enamel, Nat. Commun. 3 (1) (2012) 763, https://doi.org/10.1038/ncomms1767.
[184] Y. Lei, D. Butler, M.C. Lucking, F. Zhang, T. Xia, K. Fujisawa, T. Granzier-Nakajima, R. Cruz-Silva, M. Endo, H. Terrones, M. Terrones, A. Ebrahimi, Single-atom doping of MoS_2 with manganese enables ultrasensitive detection of dopamine: experimental and computational approach, Sci. Adv. 6 (32) (2022), eabc4250, https://doi.org/10.1126/sciadv.abc4250.
[185] I.M. Taylor, E.M. Robbins, K.A. Catt, P.A. Cody, C.L. Happe, X.T. Cui, Enhanced dopamine detection sensitivity by PEDOT/graphene oxide coating on in vivo carbon fiber electrodes, Biosens. Bioelectron. 89 (2017) 400–410, https://doi.org/10.1016/j.bios.2016.05.084.
[186] T.-C. Liu, M.-C. Chuang, C.-Y. Chu, W.-C. Huang, H.-Y. Lai, C.-T. Wang, W.-L. Chu, S.-Y. Chen, Y.-Y. Chen, Implantable graphene-based neural electrode interfaces for electrophysiology and neurochemistry in in vivo hyperacute stroke model, ACS Appl. Mater. Interfaces 8 (1) (2016) 187–196, https://doi.org/10.1021/acsami.5b08327.
[187] X. Dai, K. Le, F. Wang, R. Wei, J. Liu, Y. Jiang, H. Li, Single-molecule detection of acetylcholine by translating the neuronal signal to a single distinct electronic peak, ACS Appl. Bio Mat. 3 (10) (2020) 6888–6896, https://doi.org/10.1021/acsabm.0c00797.
[188] J. Yang, K. Zhang, J. Yu, S. Zhang, L. He, S. Wu, C. Liu, Y. Deng, Facile fabrication of robust and reusable PDMS supported graphene dry electrodes for wearable electrocardiogram monitoring, Adv. Mat. Technol. 6 (9) (2021) 2100262, https://doi.org/10.1002/admt.202100262.
[189] S. Kabiri Ameri, R. Ho, H. Jang, L. Tao, Y. Wang, L. Wang, D.M. Schnyer, D. Akinwande, N. Lu, Graphene electronic tattoo sensors, ACS Nano 11 (8) (2017) 7634–7641, https://doi.org/10.1021/acsnano.7b02182.
[190] M. Adeel, M.M. Rahman, J.-J. Lee, Label-free aptasensor for the detection of cardiac biomarker myoglobin based on gold nanoparticles decorated boron nitride nanosheets, Biosens. Bioelectron. 126 (2019) 143–150, https://doi.org/10.1016/j.bios.2018.10.060.
[191] H. Kim, Y.-T. Kwon, C. Zhu, F. Wu, S. Kwon, W.-H. Yeo, H.J. Choo, Real-time functional assay of volumetric muscle loss injured mouse masseter muscles via nanomembrane electronics, Adv. Sci. 8 (17) (2021) 2101037, https://doi.org/10.1002/advs.202101037.
[192] D.-W. Park, J.P. Ness, S.K. Brodnick, C. Esquibel, J. Novello, F. Atry, D.-H. Baek, H. Kim, J. Bong, K.I. Swanson, A.J. Suminski, K.J. Otto, R. Pashaie, J.C. Williams, Z. Ma, Electrical neural stimulation and simultaneous in vivo monitoring with transparent graphene electrode arrays implanted in GCaMP6f mice, ACS Nano 12 (1) (2018) 148–157, https://doi.org/10.1021/acsnano.7b04321.
[193] M. Zhu, X. Du, S. Liu, J. Li, Z. Wang, T. Ono, A review of strain sensors based on two-dimensional molybdenum disulfide, J. Mater. Chem. C 9 (29) (2021) 9083–9101, https://doi.org/10.1039/D1TC02102H.
[194] V. Kedambaimoole, N. Kumar, V. Shirhatti, S. Nuthalapati, P. Sen, M.M. Nayak, K. Rajanna, S. Kumar, Laser-induced direct patterning of free-standing Ti_3C_2–MXene films for skin conformal tattoo sensors, ACS Sens. 5 (7) (2020) 2086–2095, https://doi.org/10.1021/acssensors.0c00647.
[195] S. Chun, W. Son, D.W. Kim, J. Lee, H. Min, H. Jung, D. Kwon, A.H. Kim, Y.-J. Kim, S.K. Lim, C. Pang, C. Choi, Water-resistant and skin-adhesive wearable electronics using graphene fabric sensor with octopus-inspired microsuckers, ACS Appl. Mater. Interfaces 11 (18) (2019) 16951–16957, https://doi.org/10.1021/acsami.9b04206.
[196] B.-U. Hwang, J.-H. Lee, T.Q. Trung, E. Roh, D.-I. Kim, S.-W. Kim, N.-E. Lee, Transparent stretchable self-powered patchable sensor platform with ultrasensitive recognition of human activities, ACS Nano 9 (9) (2015) 8801–8810, https://doi.org/10.1021/acsnano.5b01835.
[197] F. Yin, X. Li, H. Peng, F. Li, K. Yang, W. Yuan, A highly sensitive, multifunctional, and wearable mechanical sensor based on RGO/synergetic fiber bundles for monitoring human actions and physiological signals, Sensors Actuators B Chem. 285 (2019) 179–185, https://doi.org/10.1016/j.snb.2019.01.063.
[198] Y. Pang, K. Zhang, Z. Yang, S. Jiang, Z. Ju, Y. Li, X. Wang, D. Wang, M. Jian, Y. Zhang, R. Liang, H. Tian, Y. Yang, T.-L. Ren, Epidermis microstructure inspired graphene pressure sensor with random distributed spinosum for high sensitivity and large linearity, ACS Nano 12 (3) (2018) 2346–2354, https://doi.org/10.1021/acsnano.7b07613.
[199] L.-Q. Tao, K.-N. Zhang, H. Tian, Y. Liu, D.-Y. Wang, Y.-Q. Chen, Y. Yang, T.-L. Ren, Graphene-paper pressure sensor for detecting human motions, ACS Nano 11 (9) (2017) 8790–8795, https://doi.org/10.1021/acsnano.7b02826.
[200] J. Ramírez, D. Rodriquez, A.D. Urbina, A.M. Cardenas, D.J. Lipomi, Combining high sensitivity and dynamic range: wearable thin-film composite strain sensors of graphene, ultrathin palladium, and PEDOT:PSS, ACS Appl. Nano Mat. 2 (4) (2019) 2222–2229, https://doi.org/10.1021/acsanm.9b00174.
[201] J. He, P. Xiao, J. Shi, Y. Liang, W. Lu, Y. Chen, W. Wang, P. Théato, S.-W. Kuo, T. Chen, High performance humidity fluctuation sensor for wearable devices via a bioinspired atomic-precise tunable graphene-polymer heterogeneous sensing junction, Chem. Mater. 30 (13) (2018) 4343–4354, https://doi.org/10.1021/acs.chemmater.8b01587.
[202] H. Guo, C. Lan, Z. Zhou, P. Sun, D. Wei, C. Li, Transparent, flexible, and stretchable WS_2 based humidity sensors for electronic skin, Nanoscale 9 (19) (2017) 6246–6253, https://doi.org/10.1039/C7NR01016H.
[203] L.-Q. Tao, H. Tian, Y. Liu, Z.-Y. Ju, Y. Pang, Y.-Q. Chen, D.-Y. Wang, X.-G. Tian, J.-C. Yan, N.-Q. Deng, Y. Yang, T.-L. Ren, An intelligent artificial throat with sound-sensing ability based on laser induced graphene, Nat. Commun. 8 (1) (2017) 14579, https://doi.org/10.1038/ncomms14579.
[204] W. Wu, L. Wang, Y. Li, F. Zhang, L. Lin, S. Niu, D. Chenet, X. Zhang, Y. Hao, T. F. Heinz, J. Hone, Z.L. Wang, Piezoelectricity of single-atomic-layer MoS_2 for energy conversion and piezotronics, Nature 514 (7523) (2014) 470–474, https://doi.org/10.1038/nature13792.
[205] Y. Yang, N. Huo, J. Li, Sensitized monolayer MoS_2 phototransistors with ultrahigh responsivity, J. Mater. Chem. C 5 (44) (2017) 11614–11619, https://doi.org/10.1039/C7TC03476H.
[206] Z. Yin, H. Li, H. Li, L. Jiang, Y. Shi, Y. Sun, G. Lu, Q. Zhang, X. Chen, H. Zhang, Single-layer MoS_2 phototransistors, ACS Nano 6 (1) (2012) 74–80, https://doi.org/10.1021/nn2024557.
[207] C. Choi, M.K. Choi, S. Liu, M. Kim, O.K. Park, C. Im, J. Kim, X. Qin, G.J. Lee, K. W. Cho, M. Kim, E. Joh, J. Lee, D. Son, S.-H. Kwon, N.L. Jeon, Y.M. Song, N. Lu, D.-H. Kim, Human eye-inspired soft optoelectronic device using high-density MoS_2-graphene curved image sensor array, Nat. Commun. 8 (1) (2017) 1664, https://doi.org/10.1038/s41467-017-01824-6.
[208] Y.-Z. Zhang, K.H. Lee, D.H. Anjum, R. Sougrat, Q. Jiang, H. Kim, H.N. Alshareef, MXenes stretch hydrogel sensor performance to new limits, Sci. Adv. 4 (6) (2022), eaat0098, https://doi.org/10.1126/sciadv.aat0098.
[209] Y. Wang, Z. Zeng, J. Qiao, S. Dong, Q. Liang, S. Shao, Ultrasensitive determination of nitrite based on electrochemical platform of AuNPs deposited on PDDA-modified MXene nanosheets, Talanta 221 (2021), 121605, https://doi.org/10.1016/j.talanta.2020.121605.
[210] L. Lu, X. Han, J. Lin, Y. Zhang, M. Qiu, Y. Chen, M. Li, D. Tang, Ultrasensitive fluorometric biosensor based on Ti_3C_2 MXenes with Hg^{2+}-triggered exonuclease III-assisted recycling amplification, Analyst 146 (8) (2021) 2664–2669, https://doi.org/10.1039/D1AN00178G.
[211] S.J. Kim, S. Mondal, B.K. Min, C.-G. Choi, Highly sensitive and flexible strain–pressure sensors with cracked paddy-shaped MoS_2/Graphene Foam/Ecoflex hybrid nanostructures, ACS Appl. Mater. Interfaces 10 (42) (2018) 36377–36384, https://doi.org/10.1021/acsami.8b11233.
[212] A. Harley-Trochimczyk, T. Pham, J. Chang, E. Chen, M.A. Worsley, A. Zettl, W. Mickelson, R. Maboudian, Platinum nanoparticle loading of boron nitride aerogel and its use as a novel material for low-power catalytic gas sensing, Adv. Funct. Mater. 26 (3) (2016) 433–439, https://doi.org/10.1002/adfm.201503605.
[213] X. Chen, Y.J. Park, M. Kang, S.-K. Kang, J. Koo, S.M. Shinde, J. Shin, S. Jeon, G. Park, Y. Yan, M.R. MacEwan, W.Z. Ray, K.-M. Lee, J.A. Rogers, J.-H. Ahn, CVD-grown monolayer MoS_2 in bioabsorbable electronics and biosensors, Nat. Commun. 9 (1) (2018) 1690, https://doi.org/10.1038/s41467-018-03956-9.
[214] A. Ali, O. Koybasi, W. Xing, D.N. Wright, D. Varandani, T. Taniguchi, K. Watanabe, B.R. Mehta, B.D. Belle, Single digit parts-per-billion NO_x detection using MoS_2/hBN transistors, Sensors Actuators A Phys. 315 (2020), 112247, https://doi.org/10.1016/j.sna.2020.112247.
[215] C. Zhao, X. Gan, Q. Yuan, S. Hu, L. Fang, J. Zhao, High-performance volatile organic compounds microsensor based on few-layer MoS_2-Coated photonic

crystal cavity, Adv. Optic. Materials 6 (6) (2018) 1700882, https://doi.org/10.1002/adom.201700882.
[216] S. Su, J. Li, Y. Yao, Q. Sun, Q. Zhao, F. Wang, Q. Li, X. Liu, L. Wang, Colorimetric analysis of carcinoembryonic antigen using highly catalytic gold nanoparticles-decorated MoS_2 nanocomposites, ACS Appl. Bio Mat. 2 (1) (2019) 292–298, https://doi.org/10.1021/acsabm.8b00598.
[217] H. Yang, J. Zhou, J. Bao, Y. Ma, J. Zhou, C. Shen, H. Luo, M. Yang, C. Hou, D. Huo, A simple hydrothermal one-step synthesis of 3D-MoS_2/rGO for the construction of sensitive enzyme-free hydrogen peroxide sensor, Microchem. J. 162 (2021), 105746, https://doi.org/10.1016/j.microc.2020.105746.
[218] L. Liu, S. Sang, D. Han, Z. Liu, X. Han, D. Li, Y. Chen, D. Liu, X. Liu, K. Yang, Y. Cheng, PEI/PEG functionalized Black Phosphorus prepared by a One-Pot method for a wide detection range CO_2 gas sensor, Sensors Actuators B Chem. 369 (2022), 132303, https://doi.org/10.1016/j.snb.2022.132303.
[219] J. Xu, X. Qiao, Y. Wang, Q. Sheng, T. Yue, J. Zheng, M. Zhou, Electrostatic assembly of gold nanoparticles on black phosphorus nanosheets for electrochemical aptasensing of patulin, Microchim. Acta 186 (4) (2019) 238, https://doi.org/10.1007/s00604-019-3339-3.
[220] Z. Li, Z. Yao, A.A. Haidry, Y. Luan, Y. Chen, B.Y. Zhang, K. Xu, R. Deng, N. Duc Hoa, J. Zhou, J.Z. Ou, Recent advances of atomically thin 2D heterostructures in sensing applications, Nano Today 40 (2021), 101287, https://doi.org/10.1016/j.nantod.2021.101287.
[221] H.-L. Hou, C. Anichini, P. Samorì, A. Criado, M. Prato, 2D Van der Waals heterostructures for chemical sensing, Adv. Funct. Mater. (2022), 2207065, https://doi.org/10.1002/adfm.202207065.
[222] Moving towards the market, Nat. Mater. 18 (6) (2019) 519, https://doi.org/10.1038/s41563-019-0394-4.